Temperature-driven Organization of Fish Ecosystems and Fishery Implications

Jie Li[a,b], **Matteo Convertino**[a,b*]

[a] Nexus Group, Laboratory of Information Communication Networks, Graduate School of Information Science and Technology, Hokkaido University, Sapporo, JP

[b] GI-CORE Global Station for Big Data and Cybersecurity, Hokkaido University, Sapporo, JP

January 14, 2021

Corresponding author: * M. Convertino, 9 Chome, Kita 14, Nishi 9, Kita-ku, room 11-11, Graduate School of Information Science and Technology, Hokkaido University, Sapporo, Hokkaido, Japan, 060-0814, phone: +81 011-706-6491, email: matteo@ist.hokudai.ac.jp

Keywords: fish community, abundance time series, OIF model, interaction networks, dominant eigenvalue, temperature, transitions, stability

Abstract

Fish ecosystems perform ecological functions that are critically important for the sustainability of marine ecosystems, as well as for global food security. During the 21st century, significant global warming caused by climate change has created novel challenges for fish ecosystems that threaten the global environmental and human health. Here, we study a coastal fish community in Maizuru Bay, Japan, and investigate the relationships between fluctuations of sea temperature and fish biodiversity and abundance. The global increase of temperature from 2002 to 2014 reduces fish diversity, while some species become more abundant and that causes ecological productivity to grow exponentially. The fish community is analyzed considering five temperature ranges: $\leq$10°C, 10-15°C, 15-20°C, 20-25°C, $\geq$25°C. In order to infer bidirectional interactions between species, an optimal information flow model is introduced in this study. We detect interdependencies between species and reconstruct species interaction networks that are functionally different for each temperature range. Networks for lower and higher temperature ranges are more scale-free compared to networks for the intermediate 15-20°C range in which the fish ecosystem experiences a first order phase transition from a locally stable state to a metastable state. Species-specific analysis is conducted by calculating the link salience and total outgoing information flow. Native species whose abundance is distributed more uniformly have a higher total outgoing information flow, and are the reference species (nodes in networks) of the most salient links. These species play an important role in maintaining the fish ecosystem stability. Species diversity, total interactions and entropy of species abundance in the fish community grow with the increase of temperature. This work provides a data-driven tool for analyzing and monitoring fish ecosystems under the pressure of global warming or other stressors. Macroecological and network-based analyses are useful to formulate science-based and accurate fishery policy to maintain marine fish ecosystems stable and sustainable.

1 Introduction

1.1 Impacts of Ocean Warming on Marine Fisheries

Marine fishes and invertebrates remain one of major sources of food, nutrition feeding hundreds of millions of people around the world, and have become of increasing importance, especially for coastal and developing countries, where they provide inhabitants with as much as 50% of animal protein intake (FAO, 2016). According to annual reports from FAO, global food fish consumption grew at an average rate of 3.1% from 1960s, and the average food fish consumption per capita had increased from 9.0 Kg in 1961 to 20.5 Kg in 2018, with the rate of about 1.5% per year (FAO, 2020). Despite their critical role in global food security and nutrition, fishery ecosystems are all along under increasing anthropogenic pressure from pollution, habitat degradation, overfishing and climate change that has been steadily warming the sea water. As of 2015, 33.1% of global fish stocks were assessed as fished at a rate faster than they can reproduce and therefore overexploited, while only 10% in 1974. Marine fishery ecosystems are complex systems that are highly dynamical and sensitive to external environmental factors including sea temperature. Ocean warming is altering fishery ecosystems and generally pushing negative impacts on the populations and behavior of fish species. Data from the US National Oceanic and Atmospheric Administration (NOAA) shows that sea temperature anomaly increased from -0.02°C in 1974 to 0.79°C in 2016 which is the largest anomaly observed in last 100 years (Ritchie, 2019). By comparing sea temperature data from last two decades (1999-2019) to two decades before that (1979-1999), it is observed that the rate of ocean warming had increased over 430%, meaning that ocean warming had dramatically sped up in last two decades (Ritchie, 2019; Cheng et al., 2019). "Fish are like Goldilocks: They dont like their water too hot or too cold, but just right.", said Malin L. Pinsky, a co-author of the study (Free et al., 2019), where they found that some few species populations benefited from ocean warming, but more of them suffered. Most fishes are not tolerant of abnormal fluctuations of sea temperature. From the perspective of fishery catches, ocean warming have reduced the sustainable harvest from a wide range of species by 4.1% (1.4 million metric tons of fish, approximately) since 1930s (Free et al., 2019). It has been making fish species diversity and abundance decline, and putting food supply at risk for millions of people around the world.

Due to increasing societal concerns about the sustainability of marine fish ecosystems and relevant ecological degradation under the conditions of ocean warming, assessing the vulnerability of these ecosystems to ocean warming and identifying what the sea temperature

would impose on ecosystems have received considerable interest. Currently, most studies use purely biological models to conduct these research topics on temporal scale. Through collecting and visualizing macroecological time-series data, observing the evolution of species abundance, distribution and diversity over time, and comparing macroecological evolution to the variation of oceanographic climatic data, they concluded that marine fish ecosystems are deteriorating, and one of the reasons for the deterioration is the increasing fluctuation of sea temperature caused by climate change. For example, Cheung, W. et al. found that increasingly warming sea temperature altered the composition of marine fish catches, with an increase in the proportion of warmer water species catches at higher latitudes and a decrease of subtropical species catches at lower latitudes. They plotted sea surface temperature in the past four decades and calculated mean temperature as an indicator describing the preference temperature of fish species quantified as annual fish catches of 52 large marine ecosystems (Cheung et al., 2013). Christopher M. Free et al. applied temperature-dependent population models to measure effects of ocean warming on the productivity of 235 populations of 124 species in 38 ecological regions. They analyzed the data of marine fishery production from 1930 to 2010 and computed maximum sustainable yield over time. These results addressed that maximum sustainable yield of considered fish populations decreased by 4.1% in five ecological regions experiencing losses of 15 to 35% during the studied period (Free et al., 2019). Aidan Hunter et al. used the time-series data of herring and sprat populations collected from North Sea since 1960s and west of Scotland since 1980s to identify long-term trend of species' growth rate and maturation schedules in average (Hunter et al., 2019). They visualized abundance and temperature, and estimated the trend of length at age and growth parameters including absolute growth rate over time. This study confirmed the fact that sea temperature is correlated to growth and maturation of fish species, and the mean length of herring populations steadily declined across multiple age groups. Hubert du Pontavice et al. examined influences of sea temperature on global biomass transfers from marine secondary production to fish stocks (du Pontavice et al., 2020). This study plotted the past observations of the trend of trophic transfer efficiency (TTE) and biomass residence time (BRT) in the seafood web from 1950 to 2010, and applied them to the projection of TTE and BRT by the end of the century. By visualizing the projection of TTE and BRT over time, they predicted that TTE and BRT would decrease until 2040 and remain relatively stable after 2040. All these studies, as examples, were conducted by using purely biological models on temporal scale and concluded biological results in particular fields in time domain. Results from these temporal biological models are important and valuable, but insufficient to completely describe marine fish ecosystems especially considering system dynamics and internal mechanism.

Scientists have recently paid great attention to investigating the impacts of ocean warming on marine fish ecosystems. Although conventional time-domain biological analyses are able to macroscopically display the change of fish species abundance, populations and diversity over sea temperature, it is hard to further understand how the fluctuation of sea temperature affects the collective behavior of marine fish communities, and information dynamics of ecosystems. In fact, macroscopic analyses on fish species are far from adequate to track the evolution of marine fish ecosystems under the conditions of ocean warming. In a particular fish community, there are a large number of fish species that play different roles including native and invasive species, prey and predator. In view of system, these species take various responsibilities for maintaining the marine fish ecosystem stable, and reshape the ecosystem in different ways. Therefore, investigating fish ecosystems simultaneously in temporal, systemic and species-specific sense is quite important and requisite to understand mutual relationships between fish species and sea temperature, and to find solutions to improve resilience of marine fish ecosystems to ocean warming. Purely biological analyses are incompetent to study internal responses of fish communities to the fluctuation of sea temperature in terms of system dynamics, and to specifically identify the species that are most affected by sea temperature, and most responsible for system stability. In addition, methodologies that incorporate modern information technologies and computational techniques into modeling marine fish ecosystems and relevant prediction are still lacking.

1.2 Optimal Information Flow Model and Multi-scale Ecosystem Analysis

In this study, to overcome limitations of conventional time-domain biological analyses and disentangle the complexity of mutual relationships between marine fish ecosystems and sea temperature, we develop the optimal information flow (OIF) model and employ this information-theoretic model to study a fish community in Maizuru Bay that is managed by the Maizuru Fishery Research Station of Kyoto University (Ushio et al., 2018). OIF model is based on transfer entropy (TE) that provides an asymmetric approach to measure directed information flow between random variables (species) (Schreiber, 2000; Yao and Li, 2020). It is used to infer interdependencies (defined as species interactions) between species in the fish community and reconstruct networks for describing the marine fish ecosystem, allowing us to study the ecosystem on both temporal and temperature-dependent scales in systemic way. OIF model is improved with respect to Li and Convertino (2019) by considering its extension over time to reconstruct dynamical information networks, the varied Markov order of random variables

and a refined pattern-oriented criteria to select optimal time delay and threshold based on maximization of mutual information. Therefore, OIF overcomes the limited TE for the directed uncertainty reduction scheme, for the consideration of maximum information (entropy) network (Servadio and Convertino, 2018), and MI-based maximization criteria to define the optimal time delay and interaction threshold to accurately predict systems' patterns (e.g. biodiversity). It is noteworthy to mention that the optimal threshold on interactions is not necessarily within the scale-free or maximum entropy range of inferred collective behavior. In this way, interaction processes are clearly linked to patterns which provide relevance to the inference problem. Additionally, OIF is dependent on the choice of appropriate time delay between variables for TE calculation.

Considering the fish community, in order to specifically study the effects of sea temperature on the marine fish ecosystem in view of system, long-term abundance time-series data are categorized into five groups considering five temperature ranges (TR): $\leq$10°C, 10-15°C, 15-20°C, 20-25°C, $\geq$25°C. We detect mutual relationships between species and reconstruct networks for each TR group in attempt to investigate how the fluctuations of sea temperature affect the collective behavior of particular fish species and the whole fish ecosystem by conducting network-based analyses. For each TR group, mutual causal interactions between species are inferred by OIF model (computed as TE considering optimal time delay and threshold). These OIF-inferred species interactions define the connectivity among species, forming OIF networks for all TR groups. Structural and functional patterns are recognized for OIF networks. Network-based species-specific analyses are also conducted by analyzing how much a particular species interacts others, and identifying the most salient links and critical nodes in networks. Through comparing structural and functional patterns of and critical species in networks among five TR groups, we conclude the influences of fluctuations of sea temperature on the marine fish ecosystem and its stability and identify behavioral responses to sea temperature. In particular, temperature-dependently dynamical networks are also built and analyzed to tract the evolution of the marine fish ecosystem over sea temperature. As well, since time is the most common reference system in nature, temporally dynamical networks are also implemented to capture the change of marine fish ecosystem considering long-term ocean warming. Combining with temporal biological analyses, this work is expected to give a better understanding for marine fish ecosystems that help to maintain the ecosystems stable.

1.3 Stability, Sustainability and Management of Marine Fish Ecosystems

Oceans are home to a wondrous array of plants and animals including estimated 20,000 fish species, supporting the species bank of the planet, providing humans with food consumption, and maintaining the stability of global ecosystem and environment. Although it is impossible to know the exact number of species in the ocean (scientists estimate that more than 80% of oceanic species have yet to be discovered (Mora et al., 2011)), the number of species which people already knew in the ocean is decreasing. More importantly, the rate of species extinction is still increasing, making marine fish ecosystems in trouble under ocean warming caused by anthropogenic climate change. It is urgent and important to keep marine fish ecosystems stable, sustainable and well-managed for global environment and human health. People always understand ecosystem stability in terms of biodiversity, species richness and composition, and community structure. Studying ecosystem stability only considering these biomass and taxonomic indicators is not enough. Intuitively speaking, biodiversity increases ecosystem stability, but climate change or other human-driven perturbations may alter these positive relationships (García-Palacios et al., 2018). Therefore, these relationships has been contentious. In fact, the concept of ecosystem stability is complex due to multifaceted understanding and types (Pimm, 1984; Grimm and Wissel, 1997; Loreau and de Mazancourt, 2013). As for a ecosystem, different types of stability describe different features that might lead to different patterns. Besides considering biomass and taxonomic indicators, ecosystem stability should be also explored from the perspective of the strength of species interactions, connective complex networks, topology of food webs, and resilience of species communities to different types of environmental perturbations (Ives and Carpenter, 2007).

In addition to biomass and taxonomic indicators from macroecological analyses, OIF is used to investigate ecosystem stability by inferring species interactions and reconstructing networks in this study. We macroscopically analyze the evolution of the marine fish ecosystem over sea temperature, and microscopically identify critical species who play a significant role in maintaining the structure and function of the fish ecosystem. In attempt to understand the dynamics of the fish ecosystem completely, results from biomass and taxonomic analysis and dynamical OIF interaction networks are combined together to study the fish community on multiple scales. This work would provide a potent tool to observe the stability of marine fish ecosystems, and be valuable to formulate science-based and accurate fishery policy to maintain these ecosystems stable and sustainable.

2 Materials and Methods

2.1 Fish Community Abundance Time-series Data and Categorization

Long-term time-series data (in total 285 time points) of the fish community were collected by scientists at Maizuru Fisheries Research Station, Kyoto University (Ushio et al., 2018). They conducted underwater visual census approximately every two weeks along the coast of Maizuru Bay from 1 January 2002 to 2 April 2014 (Masuda et al., 2010). Such high-frequency time series enable the detection of interactions between species. Maizuru Bay is a typical semi-enclosed water area with nearly 50m of the shore and at a water depth of 0-10m, located in the west of Wakasa Bay, Japan. Precipitation is rather high from summer to winter which is the rainy season in this area. Sea surface temperature ranged from 5.2 to 31.8, sea bottom temperature from 8.5 to 29.6, which were measured near the surface and at the depth of 10m underwater during the diving, respectively (Suzuki et al., 2019).

In this data set, only 14 dominant fish species whose total observation counts were higher than 1000, and 1 jellyfish species were included because rare species were not observed during most of census period. Rare species would bring large numbers of zeros in the time series which may lead to difficulty in analyzing data. Ignoring rare species does not significantly change the marine fish ecosystem and results of this work. Jellyfish, a non-fish species, was involved in the dataset since it was thought to have prominent influences on the dynamics of the fish community due to its large abundance. Note that time-series data were already normalized to unit mean and variance before analysis (Chang et al., 2017; Ushio et al., 2018).

In this study, we propose to study effects of water temperature on system dynamics, stability and sustainability of the fish community. To specifically do so, normalized time-series data were categorized into five subsets considering five mean temperature (the average of surface and bottom water temperature) ranges including $\leq$10°C, 10-15°C, 15-20°C, 20-25°C, $\geq$25°C, resulting in five shortened time series with 16, 93, 58, 62, 56 time points, and allowing us to separately analyze time series of these five subsets in order to disentangle how system dynamics of the fish community fluctuates with the change of sea temperature. It is worth noting that, as an assumption, the subset of time-series data after categorization in consideration of five temperature ranges are still regarded as sequential time series, called temperature-dependent time series here, even though the data categorization destroys the wholeness of original time series in terms of time order.

2.2 Probabilistic Portrayal of the Fish Community

We estimate the probability distribution of 1) the normalized abundance of fish species, and 2) inferred interactions between species (both are generally indicated as y as a generic random variable) in a way of using power-law distribution function (Barabási and Albert, 1999; Newman, 2005). Theoretically, power-law function has two types: discrete and continuous, of which the continuous form is given by (Gillespie, 2015):

$$p(y) = \frac{\varepsilon - 1}{y_{min}}(\frac{y}{y_{min}})^{-\varepsilon}, \tag{2.1}$$

where y_{min} is an estimated lower bound for which the power-law holds and $y_{min} > 0$. ε is the power-law scale exponent underlying the statistical behavior of variable studied. Power-law scale indicates how mean and variance of variables behave.

With respect to probabilistic characterization, distributions of data are visualized by computing discrete exceedance probability distribution (EPDF) that is defined as $P(Y \geq y) = 1 - P(Y < y)$, where $P(Y < y)$ is cumulative distribution function (CDF) (Gillespie, 2015) derived from probability distribution function $p(y)$ (pdf), and by plotting EPDF on log-log scale. We also introduce cutoff Y_{break} to the random variable whose probability distribution explicitly presents multiple regimes. These probability distribution regimes with different power-law scale exponents are separately estimated. Take EPDF with two regimes as an example, EPDF corresponding to this type of power-law distribution is formulated as (Convertino et al., 2013):

$$P(Y \geq y) \sim \begin{cases} (\frac{y}{y_{min}})^{-\varepsilon_1+1} f(y) & \text{for } y < Y_{break} \\ (\frac{y}{y_{min}})^{-\varepsilon_2+1} f(y) & \text{for } y \geq Y_{break} \end{cases}, \tag{2.2}$$

where Y_{break} is the break point isolating two regimes of power law distribution, $f(y)$ is a generality to formulate the cutoff (or homogeneity) function (Convertino et al., 2013), ε_1 and ε_2 are power-law scale exponents of two regimes. This type of power law is called broken power-law function, which is a piecewise function consisting of two or more components with different power-law scales in combination with particular break points (Jóhannesson et al., 2006; James et al., 2018).

2.3 Species Diversity and Abundance Characterization

To biologically observe the fish community as a local marine ecosystem, α diversity, one of the macroecological indicators, is introduced to describe the chronological fluctuation of species diversity, and how species diversity changes with the increase of temperature. Therefore, we utilize α diversity dependent on both dimensions: time and temperature, aimed at figuring out collective behavior and system dynamics of the fish community locally, temporally and spatially. α diversity referring to the biodiversity within a particular scale: period, area or ecosystem, for instance, is computed as the number of species in that scale. Given a set of unique species $\mathbf{S} = \{S_1, S_2, ..., S_n\}$ whose normalized abundances $\mathbf{X} = \{x_1, x_2, ..., x_n\}$ change over time, time-dependent α diversity $\alpha(t)$ is defined as in Li and Convertino (2019):

$$\alpha(t) = \sum_{i=1}^{n} x_i(t)^0, \tag{2.3}$$

where $x_i(t)$ is the normalized abundance of species i at the time point t. For each time point, sea surface temperature and bottom temperature were recorded. We average them as mean sea temperature and reorganize temporal α diversity considering the mean temperature corresponding to each time point, yielding temperature-dependent α diversity $\alpha(C)$.

Additionally, fish species in the fish community are distinguished into fish stocks (FS) (Begg and Waldman, 1999; Cadima, 2003), native and invasive species groups as shown in Table S1. We separately calculate the total abundance of these species groups indicated as EP (Ecological Productivity) (La Sorte et al., 2014), FS, native and invasive dependent on time and temperature using the formula:

$$A(T) = \sum_{i=1}^{n'} x_i(T), \tag{2.4}$$

where T can be time point or temperature point, $x_i(T)$ is the normalized abundance of species i at the time point T, or at the temperature point T, n' is the number of species in a particular subgroup (for all species group EP, n' is n equal to 15.).

2.4 Information-theoretical Pattern Recognition and Network Inference

2.4.1 Information-theoretical Diversity Indices and Uncertainty

Diversity indices including Shannon index ("Shannon-Wiener index") and Simpson's diversity index are statistical measures of species diversity in the fish community. They are not themselves diversities, but indices of diversity (Jost, 2006). In completely ecological sense, real diversity is an unambiguous concept recording the number of species observed at a local scale and indicating species richness and evenness. It is essential for experimentalists to document biodiversity on Earth, and ultimate reflections of disturbance driven by human activities or climate change in a particular ecosystem. This is actually what raw data can to a restricted extent do, while it is patently inadequate to dig out internal mechanisms about how ecosystems response to perturbations in terms of system dynamics and collective behavior of species. Entropy and diversity indices have a wide variety of usages under different conditions according to particular need. Entropic diversity indices are capable of providing biological information on the mechanism of assembly including rarity, commonness and fluctuation of abundance of species in fish ecosystems than real taxonomic diversity. Therefore, we calculate Shannon entropy for each species in the fish community based on probabilistic estimation of species abundance. Shannon entropy of species i is defined as $H(X_i) = -\sum_{m=1}^{v} p(x_i(m)) log_2 p(x_i(m))$, where $p(x_i(m))$ is the probability of an event m of unique normalized abundance of species i, v is the number of all unique events of abundance. Considering the whole species community, taxonomic α diversity is defined as equation 2.3. It is obvious that the sum of Shannon entropy of all species $H_\alpha = \sum_{i=1}^{n} H(X_i)$ is proportional to Shannon diversity index of the fish community, which is an information-theoretical index (Li and Convertino, 2019), defined as $H = -\sum_{i=1}^{n} p_i log_2 p_i$ (where p_i is the probability of which the species i is observed in the community). Shannon diversity index assumes that all species are regarded as a sample reservoir and species observations are sampled randomly. These information-based indices form a potent tool to understand biological mechanisms and dynamics of fish ecosystems.

2.4.2 Optimal Information Flow Model

To investigate internal mechanism and collective behavior of the fish community, we estimate mutual causal interactions between fish species. Transfer Entropy (TE), a quantity in

information theory coined in Schreiber (2000), is extensively used to measure information flow between two variables that is considered as one of the methods to quantify causal interactions. TE is mathematically defined as the amount of information that a source variable provides about the next state of a target variable in the context of the past of the target Schreiber (2000). It provides a prediction- and probabilistic-based tool in detecting directed and dynamical causal interactions without demand for any prior knowledge or assuming any particular functional form to describe the mutual interactions among elements in a dynamical system. As a result, we understand the "causal interaction" as predictability that is easier to mathematically quantified in terms of directed uncertainty reduction. The calculation of TE between two variables builds on conditional probability and joint probability considering Markov order and historical values of these variables. It is formulated as:

$$TE_{X_i \to X_j}^{(q,s,u)} = \sum_{x,y} p(x_j(t+1), x_j^{(s)}(t), x_i^{(q)}(t+1-u)) log \frac{p(x_j(t+1)|x_j^{(s)}(t), x_i^{(q)}(t+1-u))}{p(x_j(t+1)|x_j^{(s)}(t))} , \tag{2.5}$$

where X_i and X_j stand for two random variables, q and s denote the Markov order of variables X_i and X_j, $x_i(t)$ and $x_j(t)$ are time-series observations, and u is the free varied source-target time delay that yields time lagged interactions. In this study, X_i and X_j are normalized abundances of species i and j in the fish community. TE assumes that all analyzed variables obey memoryless stochastic Markov chain process (Gudivada et al., 2015). It indicates that next states of variables are only dependent on the current state, while not determined by states in the past. Thus, q and s are fixed as 1 under this assumption. TE calculation is sensitive to data features including probability distribution, extreme values and zeros. In this study, we apply Kernel (model-free) and Gaussian model (parameter-free) to test the data set of the fish community (Lizier, 2014) and compared the results with CCM model that is another well-documented algorithm to measure causal interaction between variables (Sugihara et al., 2012), and Pearson correlation coefficient (see Fig. S5). Fig. S5 shows that Kernel model provides higher resolution and gradient for TE estimation compared to Gaussian model. TE from Kernel presents similar pattern in the map (Fig. S5C) to that of CCM model (Fig. S5A) and Pearson correlation coefficient (Fig. S5B). Therefore, Kernel model is selected as the TE estimator in the OIF model.

TE is commonly used as a powerful tool to estimate mutual interactions in non-linear ecosystem thanks to its properties of inherent non-linearity, asymmetry, no model assumption (model-free) and predictability between variables (Hlavkov-Schindler et al., 2007; Vicente et al., 2011; Montalto et al., 2014; Abdul Razak and Jensen, 2014). After computing TE between species, directed interaction network visualizing the interdependencies among all

species is reconstructed from TE matrix. Networks are always hard to distinguish due to large numbers of connections. In order to reduce redundant information, we first select an appropriate time delay u that minimizes the statistical distance between species defined as equation 2.6 (Villaverde et al., 2014), equivalently maximizes the mutual information between two species.

$$d(X_i, X_j) = e^{-I(X_i;X_j)}, \tag{2.6}$$

where $I(X_i; X_j)$ is mutual information (MI) between species i and j. MI is given in information theory as:

$$I(X_i; X_j) = \sum_{x_j} \sum_{x_i} p(x_i(t), x_j(t)) log \frac{p(x_i(t), x_j(t))}{p(x_i(t))p(x_j(t))}, \tag{2.7}$$

where $p(x_i(t))$ and $p(x_j(t))$ are marginal distributions of species i and j and $p(x_i(t), x_j(t))$ is joint distribution of these two species. In this study, we specify the time delay u ranged from 0 to 10. According to equation 2.7, time delay u is selected as an integer in the range that maximizes the mutual information. It implies that u is determined by considering predictability rather than "true" causality which is strenuous to concretely estimate.

Afterwards, an appropriate value is chosen as a threshold to filter TE values. This is the second step to do the redundancy reduction by removing weak interactions (links) in networks. This step is formulated as:

$$f(X_i \to X_j) = \begin{cases} TE_{X_i \to X_j} & \text{for } TE_{X_i \to X_j} \geq TE_{thre} \\ 0 & \text{for } TE_{X_i \to X_j} < TE_{thre} \end{cases}, \tag{2.8}$$

where $f(X_i \to X_j)$ is the quantification of species interactions from species i to j, TE_{thre} is the threshold chosen to filter TE values. In this study, TE_{thre} can be a fixed value 0.01 or top 20% TE value. This two-step scenario of redundancy reduction forms the proposed optimal information flow (OIF) model.

2.4.3 Network-based Evaluation of Ecosystem Stability and Species Importance

By applying OIF model to infer species interdependence, TE matrix is obtained to quantify causal interactions between all pairs of species, and defines the structure of reconstructed networks. Firstly, we exploit eigenvalues of TE matrix as an indicator to evaluate network stability (Coyte et al., 2015; Ushio et al., 2018; Stone, 2018). Let matrix $\boldsymbol{W}$ be the TE

matrix, if there is a vector $\boldsymbol{v} \in \Re^n \neq \mathbf{0}$ that satisfies:

$$\boldsymbol{W}\boldsymbol{v} = \xi \boldsymbol{v}, \tag{2.9}$$

then scalar ξ is called the eigenvalue of $\boldsymbol{W}$ with corresponding right eigenvector $\boldsymbol{v}$. Eigenvalue is a nonzero value which can be real or complex. Real part of eigenvalues determines whether and how fast the network returns to equilibrium from a perturbation. Imaginary part of eigenvalues indicates the frequency of oscillation during the return to equilibrium.

Secondly, we evaluate ecological importance of species based on OIF network, and identify critical species in the fish community (indicated as nodes in OIF networks) using information-theoretic index and link salience measurement. The information-theoretic index is defined as total outgoing transfer entropy (OTE, computed as $OTE(i) = \sum_j TE_{i \to j}$) (Li and Convertino, 2019) that measures how much one species affects others totally. $OTE(i)$ is the total information transition from species i transmits to all other species. It can be therefore interpreted as how much one species helps to predict others in terms of predictability. OTE index is able to measure species influences with directions thanks to the asymmetric property of TE.

On the other hand, we also employ link salience that was introduced in Grady et al. (2012) to measure the importance of links in OIF networks. Link salience approach is based on the concept of effective distance $dist(i,j)$ (computed as $dist(i,j) = 1/W_{ij}$). It is intuitively assumed that strongly (weakly) interacting nodes are close to (distant from) each other. In our heterogeneous networks with real-valued weights, the algorithm of the shortest-path tree (SPT) that identifies the most efficient routes from a reference node r to the rest of the network is implemented for all nodes ($SPT(r)$). Then $SPT(r)$ is represented by a $n \times n$ matrix with element $spt_{ij}(r) = 1$ if the link (i,j) is involved in the collection of shortest paths, and $spt_{ij}(r) = 0$ if it is not. In conclusion, the link salience of OIF network is defined as:

$$SAL = \frac{1}{n} \sum_{r=1}^{n} SPT(r), \tag{2.10}$$

Therefore, SAL is a linear superposition of all $SPTs$. If the element $sal(i,j) = 0$, link (i,j) has no role in networks; if $sal(i,j) = 1$, link (i,j) is important for all reference nodes; and if $sal(i,j) = 1/2$, link (i,j) is important for only half of reference nodes (Grady et al., 2012). Node (species) importance is quantified by counting the frequency that one node exists in the most salient links as the reference terminal node (species).

2.5 Temporally and Temperature-dependently Dynamical Network Analysis

We also apply OIF model to develop dynamical networks by truncating the whole time series respectively considering time and temperature. The total number of time-series units on which dynamical network inference is carried out by OIF model is $G = \lfloor \frac{L-l}{\Delta l} \rfloor + 1$, where $\lfloor \bullet \rfloor$ rounds G to the smaller integer. When reconstructing temporally dynamical networks, L is the total number of the whole time series (here, $L = 285$), l is the length of each time-series unit, Δl is the numerical inter-observation (or time step). In this study, each time period is set as one year (the length of time-series unit l is 24 time points), time step Δl is 2 time points that correspond to one month, the whole time series is therefore truncated into 131 time-series units in total. When reconstructing temperature-dependently dynamical networks considering temperature, L is the greater integer of the maximum mean temperature, l is the upper limit of the first mean temperature range, Δl is the temperature step. In this data set, maximum mean temperature is 30.7°C (thus, L is 31). The first mean temperature range is $[6, 10]$ that means l is 10, and Δl is 1. Therefore, the whole time series is truncated into 22 time-series units corresponding to different temperature ranges whose difference is 5 except for the first temperature range $[6, 10]$. Note that the length of each time-series unit corresponding to each mean temperature range can be different.

After temporal and temperature-dependent reorganization, OIF model is used to infer species interaction (TE) matrix for each time-series unit, resulting in temporal or temperature-dependent interaction matrices $\boldsymbol{W}_{i,j}(g)$ and dynamical networks. Here, g is the time point of each time-series unit for temporally dynamical networks, while the lower limit of the temperature range for temperature-dependently dynamical networks. We analyze dynamical networks by computing total interaction (TI), dominant eigenvalues and estimated effective α diversity of each dynamical network. TI is defined as the sum of all TE values in interaction matrix $\boldsymbol{W}_{i,j}(g)$:

$$TI(g) = \sum_{i,j} \boldsymbol{W}_{i,j}(g). \tag{2.11}$$

Dynamical Stability (DS) is calculated as the absolute value of real part of dominant eigenvalue:

$$DS(g) = |Re(\xi_{max}(g))|, \tag{2.12}$$

where $\xi_{max}(g)$ is the dominant eigenvalue of an interaction matrix. Estimated effective α diversity $\alpha_e(g)$ is defined as the number of nodes (species) involved in a dynamical network

which is formulated as:

$$\alpha_e(g) = \sum_{i=1}^{n} h_i(g), \tag{2.13}$$

where

$$h_i(g) = \begin{cases} 0, & \text{for } \sum_{j=1}^{n}(|\boldsymbol{W}_{i,j}(g)| + |\boldsymbol{W}_{j,i}(g)|) = 0 \\ 1, & \text{for } \sum_{j=1}^{n}(|\boldsymbol{W}_{i,j}(g)| + |\boldsymbol{W}_{j,i}(g)|) \neq 0 \end{cases}. \tag{2.14}$$

Therefore, $\alpha_e(g)$ denotes the total number of nodes whose structural degrees are not zero in a dynamical network.

3 Results

3.1 Temporal and Temperature-driven Biomass Analysis

A simple analysis for original data of fish species abundance starts by looking into temporal trajectories and seasonal fluctuations of sea water temperature (Fig.1A), taxonomic α diversity (Fig.1B) and normalized abundance (Fig.2). It is evident that sea surface and bottom temperature, α diversity of the fish community fluctuated over time synchronously and seasonally. Approximately since 2007, seasonal fluctuations of sea surface and bottom temperature were slightly getting higher except for 2009 with the least fluctuation (Fig.1A), while the global trend of α diversity was decreasing (Fig.1B). This result means that increasing fluctuations of sea temperature lead to biodiversity loss for the fish community. The global decrease of biodiversity can be interpreted as a biological response to increasing fluctuations of sea temperature. Total abundances of EP, FS, native and invasive groups over time (Fig.2A, B) show a slight increase with fluctuations, that is opposite to the global trend of species diversity, since 2007 with the exception of a spike in 2009 and a downward spiral in 2011. The highest total abundance of species in EP, FS and native groups in 2009 is likely owing to the least temperature fluctuation in this year. This finding implies that increasing sea temperature makes some species more abundant in a global view, even though it negatively affects species diversity, and that species diversity and richness of the fish community are sensitive to the change of sea temperature, even a marginally high fluctuation. These results can be more explicitly confirmed in Fig.2C, D where total abundances of EP, FS, native, invasive groups and species 1 (*Aurelia.sp*) are observed to increase exponentially over the increasing sea temperature (Poloczanska et al., 2013; Wabnitz et al., 2018). Therein, the abundance of species 2 (*engraulis japonicus*), the one in FS group as an exception, is decreasing. Species whose abundance decreases with the increasing temperature are supposed to compete with other species and present disadvantage in species interactions. This competitive disadvantage may lead to departure and extinction of some species, resulting in the global decrease of species diversity in the fish community. We also reorganize α diversity considering sea temperature, yielding α diversity against temperature shown in Fig. 1C. It shows that α diversity grows with the increasing temperature, while the rate of the increase of α diversity ($\alpha'(C)$) gradually declines (see the black line fitting the $\alpha(C)$ points in the plot). The decreasing $\alpha'(C)$ implies that fish diversity does not continuously grow with the increase of temperature. Within lower temperature ranges, the fish community is more sensitive to the change of temperature relative to higher temperature ranges.

Time series of normalized abundance are categorized into five groups considering five temperature ranges (TRs): $\leq$10°C, 10-15°C, 15-20°C, 20-25°C, $\geq$25°C. Probability distributions of abundance data for these five TR groups are characterized by plotting EPDF on doubly logarithmic axes and estimating exponential parameters of power-law fitting (Fig.3A) (Convertino et al., 2013). EPDF plots and decreasing power-law scaling (see the subplot in Fig.3A) show that the distribution of abundance becomes more scale-free with the increase of temperature. Lower scaling of power-law fitting for higher TR groups means fatter tail of power law distribution. This indicates that the distribution of species abundance is more even since some species become abundant. These results suggest that for higher temperature, fish species present wider distribution in abundance compared to the lower temperature. Fig.3B shows standard deviation against mean abundance for each species corresponding to each TR group. Positive slopes of linear regression for these std-mean scatters address that fluctuations of species abundance scale with its magnitude. Exponents of scaling law for $\leq$10°C, 10-15°C, 15-20°C groups are higher than those of 20-25°C, $\geq$25°C groups (see the subplot in Fig.3B). This result confirms the finding from Fig. 1C that the abundance of species in lower TR groups ($\leq$10°C, 10-15°C, 15-20°C) is more sensitive to the change of temperature compared to higher TR groups (20-25°C, $\geq$25°C). Sharp decrease of scaling law implies that the fish community experiences a significant change in abundance and collective behavior around 20°C.

3.2 Interaction Inference and Temperature-dependent Network Characterization

Different patterns in EPDF and std-mean of species abundances shown in Fig.3 envision the discrepancy in species interactions and dynamics of ecosystem for different TR groups. In this study, species interaction is quantified by TE that is an information-theoretic variable measuring the amount of directed information flow and evaluating connectivity between species. Networks for the whole time series and five TR groups (see Fig.4) are therefore inferred by TE-based OIF model, and graphically visualized with *Gephi* (Bastian et al., 2009). To refine network structure, links whose TE-based interactions are lower than 0.01 are discarded by setting a threshold to filter TE. Considering the structure of networks, the size of nodes is proportional to Shannon entropy of fish species. The color of nodes linearly scales with total outgoing transfer entropy (OTE) of species: the greater the OTE of a fish species is, the warmer the color of the node. The width and color of links are proportional

to interaction between species computed as TE: the greater the TE is, the wider the link is, and the warmer links color is. The arrow of links stands for the direction of interaction (TE). Optimal Information Flow (OIF) networks present different structural and functional properties for particular TR fish groups. Network for the whole time series shown in Fig.4A provides a static overview of the fish community without considering the dynamical change of temperature or seasonality. It outlines causal relationships between species in the fish community, but is inadequate to tackle the dynamics of fish ecosystems driven by the fluctuation of temperature, and identify biological and behavioral responses. Therefore, to understand how temperature affects the fish community in detail, networks for five TR groups ($\leq$10°C, 10-15°C, 15-20°C, 20-25°C and $\geq$25°C) are reconstructed and listed in Fig.4 (from B to F). Here we first define network size as an indicator that is proportional to the number of nodes and the total amount of interactions between species. By looking at the structure of networks (Fig.4 B,C,D,E,F) and taking total interactions over temperature (Fig. S11F) into consideration, it is obviously observed that network size is larger for the fish community within a higher temperature range. Nodes connected by links with warm colors are regarded as a cluster in which species are significantly affecting others or affected by others. Network of 15-20°C group shows a larger cluster with stronger interactions between species compared to other TR groups. Yet, the distribution of species interactions in this TR group presents more evenness considering the gradient of links' color in networks. This finding can be obviously observed in Fig. 4B',C',D',E',F' describing the phase mapping of TE-based interaction matrices. TE matrix for 15-20°C group exhibits higher resolution and gradient in numeric. This result reveals that the network for 15-20°C group seems to be less scale-free versus other networks, and stands on a critical point where the fish ecosystem is experiencing a phase transition from a stable state to a metastable state. When considering specific species within different TR groups, except for the $\leq$10°C and 10-15°C groups in a globally stable state, species 6 ,7, 8, 9 are always the nodes with warm color (high OTE) (see Fig.4 A,C,D,E,F) in networks. Yet, interactions between these species are higher than others considering the phase mapping of TE matrices shown in Fig. 4. This finding means that these species are core species in the fish community that are interacting strongly with each other, present quite different dynamics in behavior compared to other species, and play a vital role in maintaining the stability of the ecosystem. It is noteworthy to mention that all these species are native species in Maizuru bay (see Table. S1).

We also set a threshold as top 20% TE considering the Pareto Principle (also known as the 80/20 rule) which specifies that roughly 80 percent of the consequences come from 20 percent of the causes in many events (Pareto, 2014). TE threshold following this rule is

generally higher than 0.01. It would further reduce network size, making inferred networks briefer relative to the networks shown in Fig.4. OIF networks (Fig.S6) for the whole time series and five TR groups with the threshold of top 20% TE are reconstructed using the same regulation used in Fig.4. After the further reduction of network size, networks in Fig. S6 ignore more functional details, but are clearer to identify the structural difference between networks compared to Fig.4. Furthermore, it is possible to statistically analyze the structural degree, in- and out-degree of nodes for each network. In Fig.S9, nodes with warm color have more links with others than others. Statistical analysis for nodal degree is shown in Fig.S7. Structural degree, in- and out-degree get higher with the increase of temperature as a whole. This result implies that warmer conditions make the fish community more socially connected. Separately, pdf of structural degree (see Fig.S7A) shows that structural degree of nodes increases with the increasing temperature, and favors bimodal distribution with different shapes for $\leq$10°C, 10-15°C, 15-20°C, 20-25°C groups, while roughly uniform distribution for $\geq$25°C group. For $\leq$10°C group, most structural degrees are distributed within the lower unimodal range from 1 to 3. With the increasing temperature, more and more values of structural degree are distributed in the higher unimodal range. However, for the highest TR ($\geq$25°C) group, the pdf of structural degree presents more evenness within the range from 0 to 10 (uniform distribution) compared to other groups. This result implies that structural degree does not increase continuously with sea temperature, and that the fish community would become less interacting when sea temperature is too high. Analogous features can be observed in the distribution of in-degree (Fig.S7B) and out-degree (Fig.S7C). For each TR group, OTE and average abundance are calculated for each species without considering any threshold for TE. Species' OTE favors bimodal distribution with short range for $\leq$10°C and 10-15°C groups, and broad range for 15-20°C, 20-25°C and $\geq$25°C groups (see Fig.S8A). This result suggests that overall effects of species on others grow with the increasing temperature. In addition, OTE is exponentially proportional to species abundance (see Fig.S8B).

3.3 Interaction Spectrum, Phase Transition and System Stability

Probability distribution of TE-based interactions is characterized by calculating discrete exceedance probability, then fitted using power-law function (see Fig.5). Among five TR groups, the greatest interaction occurs in the highest TR ($\geq$25°C) group. This result indicates that species interactions increase with sea temperature. The scaling of power-law distribution (computed as $1 - \varphi$) is lower for $\leq$10°C, 10-15°C, $\geq$25°C groups and the first regime (black fitting) of 15-20°C group compared to 20-25°C group and the second regime (green fitting) of

15-20°C group. Lower scaling of power-law fitting implies that species interactions distribute more evenly compared to those groups whose scaling of power-law fitting is higher, and that the distribution of species interactions favors more scale-free in terms of the pattern of EPDF. It is concluded that the fish community within ≤10°C and 10-15°C lies on a globally stable state. Fish community on global stability is in the situation that the fish ecosystem is highly resistant to long-term perturbations (change of species composition, sea temperature, for instance) (Nunney, 1980; CHEN and COHEN, 2001), and interspecific and intraspecific interactions are not too strong (Goh, 1977). With the increase of temperature, the fish community begins to get interacting gradually and two regimes appear in the distribution of species interactions for 15-20°C group. Therefore, the distribution of species interactions for 15-20°C group is divided into two sections by setting a break point as 0.3686 (Jóhannesson et al., 2006; James et al., 2018). Scaling exponents of these two regimes are estimated using power-law fitting separately. The first regime whose power-law scaling is lower indicates that the fish community is still partly on a globally stable state, while the second regime with a higher scaling presents a less scale-free pattern implying a metastable state. This result suggests that for 15-20°C temperature range, the fish community stands on a critical point where the fish ecosystem is experiencing a phase transition from global stability to metastability, and that the collective behavior of species is experiencing a significant change driven by sea temperature. The change of collective behavior can be reflected by fluctuations of species diversity and abundance. For example, a significant drop (transition) of scaling law is observed in standard deviation against mean abundance as temperature rises from 15-20°C to 20-25°C (see Fig.3B). The power-law fitting for the second regime of 15-20°C group and 20-25°C group is the highest scaling among five TR groups. It suggests that major species interactions continue to increase as temperature rises, and large numbers of minor species interactions emerge simultaneously, leading to a distribution pattern that most interactions are clustered within a lower range. This distribution pattern of the fish ecosystem implies a less scale-free state compared to other TR groups. Fish ecosystems within 15-20°C and 20-25°C are therefore metastable (also see Fig.4D,E,D',E'). With the continuous increase of temperature (≥25°C), the power-law scaling of the species interaction distribution shows a significant decrease that is opposite to sea temperature. This result indicates that several major species interactions continue to rise, while minor interactions disappear, leading to a flatter distribution and more scale-free pattern compared to 15-20°C and 20-25°C groups. The fish ecosystem returns to another stable state after fluctuations caused by sea temperature. This finding confirms the fact that the fish community would not get interacting continuously with the increase of sea temperature, yet the activity of fish species would

decrease when temperature is too high. This newly established stable state is interpreted as locally stable state which addresses the fish ecosystem only resistant to small short-lived disturbances (minor fluctuation of sea temperature, for instance) (Ak Gümüs, 2014). By connecting scaling exponents of the power-law fitting for TR groups over sea temperature shown in Fig.5F, the trend of power-law exponents also explicitly shows that the dynamical fish ecosystem is subjected to phase transition from global stability to metastability, and finally returns to local stability with the increase of temperature. A bifurcation occurs considering the division of species interaction distribution for 15-20°C group. This result reveals that, during the phase transition from global stability to local stability, the fish ecosystem stands at a critical point within 15-20°C where the fish community experiences a significant change in collective behavior. These changes result in different structural and functional features for the fish ecosystem within different temperature ranges graphically shown in OIF networks (see Fig.4).

Eigenvalues and eigenvectors provide essential information for reflecting the stability of dynamical systems (Woolf, 2009). Generally, differential equations are used to mathematically describe system dynamics based on variables in the particular system, and eigenvalues and eigenvectors can be used as a method to solve differential equations. The real part of eigenvalues determines whether the system is stable, and the imaginary part determines whether the oscillation is damped or not. If the real part of eigenvalues is negative, the system is stable and damped if the imaginary part is also negative, while undamped if the imaginary part is positive. If the real part of eigenvalues is positive, the system is unstable (Woolf, 2009). In this study, the eigenvalues of each interaction matrix corresponding to each TR group are scattered together in a complex plane (Fig. 6). This method displays the position of all eigenvalues in the form of an ellipse (Coyte et al., 2015; Stone, 2018). If only considering the eigenvalues with positive real part that may result in instability, Fig. 6 shows one eigenvalue with the lowest positive real part for ≤10°C group, no eigenvalue with positive real part for 10-15°C group, two eigenvalues with positive real part for 15-20°C group, one eigenvalue with a positive real part for 20-25°C while lower than that for 15-20°C group, and one eigenvalue with the largest positive real part for ≥25°C group. These results highlight that the fish ecosystem within low sea temperature ranges (≤10°C and 10-15°C) is stable, while becomes more interacting, leading to an unstable or metastable state as the sea temperature rises, especially for the 15-20°C group which has two eigenvalues with positive real part.

3.4 Network-based Biological Importance and Critical Species Identification

Biological importance and critical species identification are performed by further analyzing structural features of OIF networks and combining interaction spectrum with abundance spectrum. To this end, we first measure the salience for all links in OIF networks (Grady et al., 2012). Link salience computation is based on the effective proximity d_{ij} defined by the strength of mutual interactions: $d_{ij} = 1/TE_{ij}$. It is intuitively assumed that strongly (weakly) interacting nodes are close to (distant from) each other. Link salience matrices shown in Fig. 7 illustrate that species 7 (*Pseudolabrus.sieboldi*) is always the reference node of the most salient links with the exception of $\leq$10°C group where the reference node of the most salient links is species 15 (*Rudarius.ercodes*) instead of species 7. According to the website of *fishbase* (`http://www.fishbase.org/summary/Pseudolabrus-sieboldi.html`), species 7 (*Pseudolabrus.sieboldi*) is a native species in northwest pacific ocean and mainly distributed in Japan waters (Mabuchi et al., 2007). These results reveal that native species 7 has the most critical influence on other species in the fish community, and plays a vital role in maintaining structure and function of networks.

We also calculate Shannon entropy for species to measure the fluctuation and uncertainty of species abundance, and compute species' OTE as another nodal (species) property to quantify how much a species totally influences others in OIF networks. Then, species rankings considering top 5 Shannon entropy and top 5 OTE are listed and shown in Fig.S9. On the one hand, the species ranking of Shannon entropy (left figures in Fig.S9) shows that species 2 or (and) 5 always have the greatest Shannon entropy that represents the highest uncertainty in abundance for these two species. This finding also can be observed in the original time series of abundance plotted in Fig.S3. Species 2 and 5 have the highest fluctuation of abundance and the most diverse events in numeric. On the other hand, the species ranking of OTE (right figures in Fig.S9) shows that for all TR groups except the $\leq$10°C group, species 7 always has the greatest OTE, and species 6, 7, 8 and 9 are are often involved in top 5 OTE ranking for 15-20°C, 20-25°C and $\geq$25°C groups. This finding means that these species have significant effects on other species in the fish community, of which species 7 is the greatest. This result is in accordance with the results of link salience matrices shown in Fig.7. In a word, through measuring link salience and OTE, species 6, 7, 8, 9 can be identified as the critical species in the fish community. Moreover, probability distribution functions of abundance for all species (see Fig.S2) show that normalized species abundances of these species are more evenly distributed within relatively small ranges (the least range is [0,45) for species

7) compared to other species with wide distributions and extreme values. It demonstrates that trajectories of species abundance for species 6, 7, 8 and 9 are remarkably divergent from other species. Species with wide distributions and extreme values present more uncertainty in abundance, that is, Shannon entropy of these species is higher than that of species 6, 7, 8, 9. Transfer entropy from source variables (species) with low uncertainty in abundance (species 6, 7, 8, 9, for instance) to target variables with high uncertainty (see left figures in Fig.S9) is supposed to be high. Considering species 6, 7, 8 and 9 themselves, within the small range of abundance distribution, relatively speaking, these species also present transparent divergences (dissimilarity) in the distribution of species abundance. Therefore, mutual interactions (transfer entropy) between these species are relatively high. These results address that the distribution of species abundance can be used as a proxy of interactions by comparing similarity and divergence. Take species 2 (*Engraulis.japonicus*) as an extreme example, TEs from species 2 to others are expected to be low since original abundance data of species 2 have many zeros or values close to zero that lead to lower uncertainty despite the asynchrony and divergence.

Considering the whole time series, rather than solely estimate the simple continuous pdf of abundance for each species (Fig.S2), we probabilistically characterize distributions of abundance by computing EPDF and using power-law fitting. The scaling exponent of power-law fitting is considered as another species property in terms of the distribution of taxonomic abundance (see Fig.S1). Thereafter, abundance-interaction phase space describing relationships between power-law scaling and species OTE (power-law exponents vs. OTE for all species, indeed) is shown in Fig. 8. For a particular species, the greater the exponent of power-law fitting for the EPDF is, the more the abundance values are distributed within a lower range; the higher the OTE is, the stronger the species interacts others. The phase space mapping shows a rough trend as a whole that the exponent of power-law fitting for the EPDF of species abundance is proportional to the species OTE with the exceptions of species 3 and 6. This result suggests that species whose abundance has a wide distribution with a fat tail have relatively low total effects on other species, while species whose abundance is evenly distributed within a narrow range have high total effects on other species (species 7, 8, 9, 10 in the figure, for instance). These findings are also observed in the phase mapping of interaction matrix for the whole time series shown in Fig. 4A'. It is intuitively speculated that species with more uniform distribution play a cooperative role in the fish community that is beneficial to the increase of abundance, but do not have strong effects on other species. In Fig.S10, OTE vs. mean abundance shows that for most species, effects on other fishes are proportional to the abundance of species (Fig.S10A), while inversely proportional to the

standard deviation of the abundance of species (Fig.S10B). This result implies that native species with relatively uniform distribution of abundance play a significant role in the fish community.

Additionally, to identify which species are most affected by sea temperature, TE, MI, species abundance vs. sea temperature, Pearson correlation coefficient (indicated as cc) and ρ of CCM (Sugihara et al., 2012) are used as indicator to measure the relationship between species abundance and sea temperature (Table 1). Note that the indicator of slope is the exponent of exponential fitting for species abundance vs. sea temperature (see Fig.S4). In table 1, TE from sea temperature to species abundance for species 5, 6 and 7 is higher than other species, yet MI, Pearson correlation coefficient and ρ are overall higher for species 5, 6, 7, 8 and 9. Species 5, 6, 7, 8 and 9 are therefore considered as the species that are most affected by sea temperature. By looking into Fig.S4, the abundance of species 5, 6, and 7 exponentially scales with sea temperature more obviously than other species. These results mean that OIF-inferred TE outperforms other indicators for this purpose. TE values from species abundance to sea temperature are very small. It is intuitively understandable that fish species in the ocean do not affect environmental factors (Ushio et al., 2018).

3.5 Temporally and Temperature-dependently Dynamical Interactions and Stability

Considering both dimensions of time and temperature, temporally and temperature-dependently dynamical species interaction (TE) matrices are inferred from time series of each time and temperature unit, respectively. On the temporal scale, Fig. S11A shows the real part of the dominant eigenvalue of TE matrix (blue line) and adjacency matrix (red line) underlying the structure of temporally dynamical networks. The real part of the dominant eigenvalue of TE matrix over time is lower than that of adjacency matrix, yet the former presents an obvious seasonal fluctuation. In the first half-year period (approx. from winter to early summer), it is observed that the real part of the dominant eigenvalue increases over time and reaches a spike during this period. Then it decreases in the second half-year period, while increases again at the end of year. The increasing trend or the high level of the real part of the dominant eigenvalue always appears within the time period with higher changes (fluctuations) of sea temperature (from April to June or from October to December) in a year which probably corresponds to 15-20°C to 20-25°C temperature ranges. These results suggest that the fluctuation of species interactions becomes higher and fluctuates more frequently during the

time period with higher fluctuations of sea temperature, and that the fish ecosystem tends to be metastable as the fish community becomes active. For adjacency matrix, the high level of the real part of the eigenvalue appears synchronously with that of TE matrix, while it is hard to identify the seasonality due to lower fluctuations. Fig. S11B shows the magnitude of total interactions over time that is computed as the sum of TE values in interaction matrices of temporally dynamical networks. Total interaction over time presents clear seasonal fluctuations that highly synchronize with the seasonality observed in eigenvalues of TE matrix shown in Fig. S11A (blue line). This finding verifies the result that species interactions in the fish community increase during the time period with high fluctuations of sea temperature. Furthermore, species OTE is calculated for each temporally dynamical network, obtaining 256 OTEs for each species. Pdfs of species OTE show that critical species 6, 7, 8, 9 have higher effects on other species in the fish community compared to others (see Fig. S12).

On the scale of temperature, Fig. S11E shows how the real part of the dominant eigenvalue of TE matrix (blue line) and adjacency matrix (red line) underlying the structure of temperature-dependently dynamical networks changes with the increase of temperature, respectively. Both curves show that the real part of the dominant eigenvalue rises with the increasing temperature as a whole, while that of TE matrix has more informative fluctuations with higher frequency relative to adjacency matrix. Fig. S11F shows the magnitude of total interaction over temperature stemmed from TE matrices of temperature-dependently dynamical networks. It is clearly observed that total interactions analogously fluctuate with the real part of the dominant eigenvalue of TE matrix shown in Fig. S11E, as well as to the estimated effective α diversity over temperature derived from dynamical TE-based interaction matrices after filtering by top 20% TE shown in Fig. S11H. From the perspective of network-based models, these results indicate that quantitative interactions between species in the fish community are more sensitive to fluctuations of sea temperature compared to macroecological α diversity. The fluctuation of species interactions provides a potent strategy to monitor and predict biological collective behavior and system dynamics of the fish community, especially for internal intra- and inter-specific mechanisms and their responses to the change of environmental factors. The effective α diversity in temporal and temperature-dependent dimensions is shown in Fig. S11C,D,G,H.

4 Discussion

Growth, reproduction and living habits of organisms in the ocean, as well as external environmental factors including sea temperature and daytime present a transparent seasonality. Therein, sea temperature is often perceived as a dominant ingredient that drives the biological behavior of organisms in ecosystems (Dangles et al., 2008; Kitayama et al., 2020), while also affected by human-induced climate change. For marine fish ecosystems, as narrated in the part of introduction, ocean warming has been pushing significant negative impacts on marine ecosystems and fish species. In this paper, we study the multispecies fish community in Maizuru bay by conducting biomass and taxonomic analyses on temporal scale first. These analyses capture the seasonal fluctuations of sea temperature, species diversity and abundance and conclude that the increasing fluctuations of sea temperature result in global biodiversity loss. Particularly, biomass and taxonomic analyses are also conducted on temperature scale considering five temperature ranges to investigate how sea temperature affects the fish community in biomass and taxonomy. Temperature-dependent analyses capture the difference in macroecological indicators of the fish community among five TR groups. In addition, same analyses for EP, FS, native and invasive groups and two species (species 1 and 2) are performed to identify cooperative or competitive interactions in the fish community. The result is helpful to explain the finding that species diversity loses even though the abundance of some fish species grows under ocean warming. Some valuable results are obtained from the analysis considering species abundance and diversity, while it is not sufficient to completely display the impacts of sea temperature on the fish community, and limited to describe internal mechanisms of how sea temperature affects the dynamics of the fish ecosystem.

To better understand biological responses of the fish community to the fluctuations of sea temperature, the proposed information-theoretic OIF is employed to study the fish community considering species interactions and system dynamics. In information theory that has attracted attention in complex networks research, entropy (information) is used to quantify the uncertainty of a variable and its computation is based on the distribution of observations. Transfer entropy is an asymmetric variable that measures directed relationships between two random variables by estimating the directed information flow between variables. In complex ecosystems, the concept of entropy is also used as indices for measuring diversity (Shannon-Wiener and Gini-Simpson diversity, for instance) (Jost, 2006). The fundamental work of studying complex ecosystems is to detect complex interdependencies comprised of a large number of potential interactions between all species. Therefore, the intuitive and heuristic notion in information theory for species interaction detection is transfer entropy. Therefore,

OIF model is introduced and deployed in this study to detect potential species interactions that form information flow networks modeling the fish ecosystem. Networks inferred from OIF model illustrate differences in structure and function among five TR groups. These structural and functional differences imply different system states and dynamics the fish community presents within different temperature ranges. For the lowest temperature range, the fish community lies on a globally stable state, then changes the state to metastability in intermediate temperature ranges, and finally returns to a locally stable state. As well, different patterns are recognized for internal mechanisms of the fish ecosystem within different temperature ranges by probabilistically characterizing species interactions. These shifts of ecosystem state and dynamics explain how sea temperature substantially affects the fish community. In addition, eigenvalues of TE-based interaction matrix are computed as indices to asses the ecosystem stability of the fish community (Coyte et al., 2015; Stone, 2018). The determination of eigenvalues and eigenvectors of a system is extremely important to many problems in physics and engineering including stability analysis, oscillations of vibrating systems, to name only a few. It provides three measures of stability in terms of species interactions: (i) whether the fish community will return to the previous state after a certain perturbation, (ii) how fast the return will occur, and (iii) what the interactome dynamics of the fish community look like during the process of the return.

It is important to note that different species may respond to the fluctuation of sea temperature in different ways. As one of the factors, these different behavioral responses improve the complexity of fish ecosystems, and could be exponentially proportional to the number of species in the fish community. To further tackle the complexity of system dynamics and identify the roles and importance of some critical species under the conditions of ocean warming, species-specific analyses are conducted by doing network-based computation and combining the network-based results with species diversity and abundance information. Firstly, link salience estimation is used as network-based analyses to classify the salient links in complex networks based on a consensus estimate of all nodes (Grady et al., 2012). Here, we also apply this algorithm to identify critical species in the fish community by finding the common species in the classified salient links. Native species 7 (*Pseudolabrus.sieboldi*) is the most frequently observed species in the salient links as a reference node. This result means that species 7 is likely to play a more significant role in maintaining the fish ecosystem stable compared to other species. Secondly, OTE that counts the total effects of one species on others is calculated for each species as a nodal property in networks. TE and OTE are considered as the strong indicators of ecosystem dynamics for pairwise and nodal functional characterization since those variables are related to species interdependence in view of complex networks (Li

and Convertino, 2019). These information-theoretic indicators based on the interdependence between species rather than pure biological species values lead to more informative biological meaning and offer better characterization and understanding for networks and their dynamical evolution. From the perspective of uncertainty reduction and predictability, it can be also said that TE measures how much the source variable helps to predict the target. Therefore, OIF-inferred networks are interpreted as predictive interaction networks, and OTE is a variable measuring how much one species contributes to the prediction of next states of the fish ecosystem. From this framework, species 6, 7, 8 and 9 are identified as critical species often involved in top 5 OTE ranking, and species 7 has the greatest OTE for all TR groups, but the $\leq$10°C group. This finding coincides with the results from salient link classification. In consideration of biomass and taxonomic analyses, the abundance of species 6, 7, 8 and 9 presents remarkable divergence from other species (see Fig.S2 and S3). For two divergent variables, TE from source variable with lower uncertainty to the target with higher uncertainty is supposed to be high. By combining these results together, it addresses that the distribution of species abundance can be used as a proxy of interactions in terms of divergence, asynchronicity and diversity of events.

We also develop dynamical networks dependent on time and temperature. In consideration of the relationship between eigenvalues and system stability, species interactions and effective diversity indicators, network-based analyses including the real part of the dominant eigenvalue of TE matrices, total interaction of dynamical networks and estimated effective α diversity are implemented in this section. Dominant eigenvalues over time reveal that the fish ecosystem is less stable (metastable) during the period with higher fluctuations of sea temperature in one year. This result is in line with the metastable state of 10-15°C and 15-20°C groups concluded in section 3.3, since these two temperature ranges are more likely to appear in spring and autumn which have relatively high temperature fluctuations in one year. Dominant eigenvalues over temperature also suggest that in a certain temperature range ($\leq$18°C), the increasing temperature rapidly makes the fish ecosystem more interacting, but less stable. Total interaction of dynamical networks present equivalent fluctuations to eigenvalues on both scales that explicitly imply the relationship between species interaction and system stability. Moreover, effective α diversity from OIF networks is able to roughly track the real taxonomic diversity. Therefore, dynamical network analyses provide a real-time and temperature-dependent monitor that could directly display the system states and species activeness in view of system dynamics. This is important and useful to understand how the fish ecosystem responds to the change of sea temperature especially in the conditions of ocean warming, and to keep the fish community well-managed and stable.

5 Conclusions

Temperature is one of the dominant environmental factors that drives marine fish ecosystems and collective behavior of fish species. Abnormal fluctuations of sea temperature caused by climate change have created significant challenges for fish ecosystems (Brierley and Kingsford, 2009). In this study, the fish community in Maizuru Bay is studied in the time domain, as well as on temperature scale by considering biomass and taxonomy, species interactions and complex systems, and network-based species-specific identification.

- Time-domain analyses of biomass and taxonomy present seasonal fluctuations of sea temperature and α diversity. Slightly increasing fluctuations of sea temperature are observed in the figure of temperature vs. year, while the global level of species diversity decreases. Accordingly, the increasing fluctuations of sea temperature may lead to the biodiversity loss in the fish community. Total abundance of species in EP, FS, native and invasive groups slightly increases over year, and exponentially increases with the increase of sea temperature considering temperature scale. These findings indicate that increasing sea temperature leads to the rise of species abundance, even though it brings biodiversity loss in a global view. Biomass and taxonomic analyses for five TR groups show that species abundance is distributed more evenly for higher TR group, and the variance of species abundance scales with its magnitude. On temperature scale, taxonomic α diversity grows with the increasing temperature, and is more sensitive to the change of temperature for lower TR groups.

- We introduce OIF model to infer species interactions in the fish community, and reconstruct OIF networks for the whole time series and five TR groups. OIF network for 15-20°C group seems to be less scale-free vs. other networks, indicating that the fish ecosystem within this temperature range is on critical metastable state, and experiencing phase transition from local stability ($\leq$10°C group) to metastability. In addition, collective behavior of species undergoes a significant change. From $\leq$10°C to $\geq$25°C group, nodal degree increases, but not consecutively when sea temperature continues to rise. High sea temperature makes the fish community socially connected, while would return to be silent when sea temperature is too high.

- Network-based analyses for species-specific identification based on the algorithm to classify salient links and OTE framework reveal that species 7 (*Pseudolabrus.sieboldi*) is likely to have the greatest influence on other species in the fish community and play a more important role in maintaining the stability of the fish ecosystem. OTE framework

also recognizes a cluster involving species 6, 7, 8 and 9 that strongly interact each other. Note that species abundance of these species is remarkably divergent from others (see Fig.S2 and S3). It is concluded that the distribution of species abundance can be a proxy of species interaction in terms of divergence, asynchronicity and diversity of events.

- Temporally dynamical networks present the seasonality of stability. During the time period with high fluctuations of temperature (spring or autumn, for instance) in one year, the real part of the dominant eigenvalue of TE-based interaction matrix is high, suggesting that the fish community is more interacting and becomes metastable. Considering temperature-dependently dynamical networks, the real part of the dominant eigenvalue over temperature increases in a certain temperature range ($\leq$18°C). The increasing temperature makes the fish ecosystem more interacting, but less stable. The fluctuation of total interaction of dynamical networks is highly synchronous with that of the real part of the dominant eigenvalue. Effective α diversity from dynamical OIF networks is able to roughly track the taxonomic α diversity. Species interaction is more sensitive to the fluctuation of sea temperature compared to effective and taxonomic α diversity.

This study provides a two-dimensional (time and temperature) analysis for studying the fish community considering biomass and taxonomy, and system dynamics, respectively. Conventional time-domain analysis for biomass and taxonomy highlights the seasonal fluctuation of alpha diversity and species abundance. OIF model allows to investigate the fish community in view of species interactions and system dynamics. By reconstructing OIF networks, we study the evolution of ecosystem stability by analyzing structural and functional features of these networks. Network-based species-specific analyses are also conducted to identify critical species and clusters in the fish community, which might be most affected by the fluctuation of sea temperature, and responsible for keeping the fish ecosystem stable. Therefore, this work is important and useful to completely understand marine fish ecosystems and their responses to the fluctuation of sea temperature. It would be helpful to formulate science-based and accurate fishery policy to protect marine ecosystems and improve system resilience to ocean warming caused by climate change.

Acknowledgments

M.C. and J.L. gratefully acknowledge the funding provided by the GI-CORE Global Station for Big-Data and Cybersecurity at Hokkaido University, Sapporo, JP. M.C. acknowledges the FY2020 SOUSEI Support Program and Award for Young Researchers awarded by the Executive Office for Research Strategy to the Top 20% scientists in terms of productivity and citations at Hokkaido University. M.C. also acknowledges the Microsoft AI for Earth computational resources and the NIH funded Big Data to Knowledge (BD2K) 2017 Innovation Lab Quantitative Approaches to Biomedical Data Science Challenges in our Understanding of the Microbiome managed by the BD2K Training Coordinating Center (TCC).

Author Contribution

J. L. and M.C. idealized the study and wrote the manuscript. J.L. made all calculations.

References

Fatimah Abdul Razak and Henrik Jeldtoft Jensen. Quantifying causality in complex systems: Understanding transfer entropy. PLOS ONE, 9(6):1–14, 06 2014. doi: 10.1371/journal.pone.0099462. URL https://doi.org/10.1371/journal.pone.0099462.

Özlem Ak Gümüs. Global and local stability analysis in a nonlinear discrete-time population model. Advances in Difference Equations, 2014(1):299, 2014. ISSN 1687-1847. doi: 10.1186/1687-1847-2014-299. URL https://doi.org/10.1186/1687-1847-2014-299.

Albert-László Barabási and Réka Albert. Emergence of scaling in random networks. Science, 286(5439):509–512, 1999. ISSN 0036-8075. doi: 10.1126/science.286.5439.509. URL https://science.sciencemag.org/content/286/5439/509.

Mathieu Bastian, Sebastien Heymann, Mathieu Jacomy, et al. Gephi: an open source software for exploring and manipulating networks. Icwsm, 8(2009):361–362, 2009.

Gavin A Begg and John R Waldman. An holistic approach to fish stock identification. Fisheries research, 43(1-3):35–44, 1999.

Andrew S Brierley and Michael J Kingsford. Impacts of climate change on marine organisms and ecosystems. Current biology, 19(14):R602–R614, 2009.

Emygdio L Cadima. Fish stock assessment manual. Number 393. Food & Agriculture Org., 2003.

Chun-Wei Chang, Masayuki Ushio, and Chih-hao Hsieh. Empirical dynamic modeling for beginners. Ecological Research, 32(6):785–796, Nov 2017. ISSN 1440-1703. doi: 10.1007/s11284-017-1469-9. URL https://doi.org/10.1007/s11284-017-1469-9.

XIN CHEN and JOEL E. COHEN. Global stability, local stability and permanence in model food webs. Journal of Theoretical Biology, 212(2):223 – 235, 2001. ISSN 0022-5193. doi: https://doi.org/10.1006/jtbi.2001.2370. URL http://www.sciencedirect.com/science/article/pii/S0022519301923707.

Lijing Cheng, John Abraham, Zeke Hausfather, and Kevin E. Trenberth. How fast are the oceans warming? Science, 363(6423):128–129, 2019. ISSN 0036-8075. doi: 10.1126/science.aav7619. URL https://science.sciencemag.org/content/363/6423/128.

William W. L. Cheung, Reg Watson, and Daniel Pauly. Signature of ocean warming in global fisheries catch. Nature, 497(7449):365–368, May 2013. ISSN 1476-4687. doi: 10.1038/nature12156. URL https://doi.org/10.1038/nature12156.

Matteo Convertino, Filippo Simini, Filippo Catani, Igor Linkov, and Gregory A. Kiker. Power-law of aggregate-size spectra in natural systems. EAI Endorsed Trans. Complex Systems, 1:e2, 2013.

Katharine Z. Coyte, Jonas Schluter, and Kevin R. Foster. The ecology of the microbiome: Networks, competition, and stability. Science, 350(6261):663–666, 2015. ISSN 0036-8075. doi: 10.1126/science.aad2602. URL https://science.sciencemag.org/content/350/6261/663.

O. Dangles, C. Carpio, A. R. Barragan, J.-L. Zeddam, and J.-F. Silvain. Temperature as a key driver of ecological sorting among invasive pest species in the tropical andes. Ecological Applications, 18(7):1795–1809, 2008. doi: 10.1890/07-1638.1. URL https://esajournals.onlinelibrary.wiley.com/doi/abs/10.1890/07-1638.1.

Hubert du Pontavice, Didier Gascuel, Gabriel Reygondeau, Aurore Maureaud, and William W. L. Cheung. Climate change undermines the global functioning of marine food webs. Global Change Biology, 26(3):1306–1318, 2020. doi: 10.1111/gcb.14944. URL https://onlinelibrary.wiley.com/doi/abs/10.1111/gcb.14944.

FAO. The state of world fisheries and aquaculture 2020. sustainability in action. Food and Agriculture Organization of the United Nations, 2020.

UN FAO. The state of world fisheries and aquaculture 2016. contributing to food security and nutrition for all. 2016.

Christopher M. Free, James T. Thorson, Malin L. Pinsky, Kiva L. Oken, John Wiedenmann, and Olaf P. Jensen. Impacts of historical warming on marine fisheries production. Science, 363(6430):979–983, 2019. ISSN 0036-8075. doi: 10.1126/science.aau1758. URL https://science.sciencemag.org/content/363/6430/979.

Pablo García-Palacios, Nicolas Gross, Juan Gaitán, and Fernando T. Maestre. Climate mediates the biodiversity–ecosystem stability relationship globally. Proceedings of the National Academy of Sciences, 115(33):8400–8405, 2018. ISSN 0027-8424. doi: 10.1073/pnas.1800425115. URL https://www.pnas.org/content/115/33/8400.

Colin Gillespie. Fitting heavy tailed distributions: The powerlaw package. Journal of Statistical Software, Articles, 64(2):1–16, 2015. ISSN 1548-7660. doi: 10.18637/jss.v064.i02. URL https://www.jstatsoft.org/v064/i02.

B. S. Goh. Global stability in many-species systems. The American Naturalist, 111(977):135–143, 1977. URL http://www.jstor.org/stable/2459985. Full publication date: Jan. - Feb., 1977.

Daniel Grady, Christian Thiemann, and Dirk Brockmann. Robust classification of salient links in complex networks. Nature Communications, 3(1):864, May 2012. ISSN 2041-1723. doi: 10.1038/ncomms1847. URL https://doi.org/10.1038/ncomms1847.

V. Grimm and Christian Wissel. Babel, or the ecological stability discussions: an inventory and analysis of terminology and a guide for avoiding confusion. Oecologia, 109(3):323–334, Feb 1997. ISSN 1432-1939. doi: 10.1007/s004420050090. URL https://doi.org/10.1007/s004420050090.

Venkat N Gudivada, Dhana Rao, and Vijay V Raghavan. Big data driven natural language processing research and applications. In Handbook of Statistics, volume 33, pages 203–238. Elsevier, 2015.

Katerina Hlavkov-Schindler, Milan Palu, Martin Vejmelka, and Joydeep Bhattacharya. Causality detection based on information-theoretic approaches in time series analysis. Physics Reports, 441(1):1 – 46, 2007. ISSN 0370-1573. doi: https://doi.org/10.1016/j.physrep.2006.12.004. URL http://www.sciencedirect.com/science/article/pii/S0370157307000403.

Aidan Hunter, Douglas C. Speirs, and Michael R. Heath. Population density and temperature correlate with long-term trends in somatic growth rates and maturation schedules of herring and sprat. PLOS ONE, 14(3):1–22, 03 2019. doi: 10.1371/journal.pone.0212176. URL https://doi.org/10.1371/journal.pone.0212176.

Anthony R. Ives and Stephen R. Carpenter. Stability and diversity of ecosystems. Science, 317(5834):58–62, 2007. ISSN 0036-8075. doi: 10.1126/science.1133258. URL https://science.sciencemag.org/content/317/5834/58.

Charlotte James, Sandro Azaele, Amos Maritan, and Filippo Simini. Zipf's and taylor's laws. Phys. Rev. E, 98:032408, Sep 2018. doi: 10.1103/PhysRevE.98.032408. URL https://link.aps.org/doi/10.1103/PhysRevE.98.032408.

Gudlaugur Jóhannesson, Gunnlaugur Bjrnsson, and Einar H. Gudmundsson. Afterglow light curves and broken power laws: A statistical study. The Astrophysical Journal, 640(1): L5–L8, feb 2006. doi: 10.1086/503294. URL https://doi.org/10.1086%2F503294.

Lou Jost. Entropy and diversity. Oikos, 113(2):363–375, 2006. doi: 10.1111/j.2006.0030-1299.14714.x. URL https://onlinelibrary.wiley.com/doi/abs/10.1111/j.2006.0030-1299.14714.x.

Kanehiro Kitayama, Masayuki Ushio, and Shin-Ichiro Aiba. Temperature is a dominant driver of distinct annual seasonality of leaf litter production of equatorial tropical rain forests. Journal of Ecology, n/a(n/a), 2020. doi: 10.1111/1365-2745.13500. URL https://besjournals.onlinelibrary.wiley.com/doi/abs/10.1111/1365-2745.13500.

Frank A. La Sorte, Daniel Fink, Wesley M. Hochachka, John P. DeLong, and Steve Kelling. Spring phenology of ecological productivity contributes to the use of looped migration strategies by birds. Proceedings of the Royal Society B: Biological Sciences, 281(1793): 20140984, 2014. doi: 10.1098/rspb.2014.0984. URL https://royalsocietypublishing.org/doi/abs/10.1098/rspb.2014.0984.

Jie Li and Matteo Convertino. Optimal microbiome networks: Macroecology and criticality. Entropy, 21(5), 2019. ISSN 1099-4300. doi: 10.3390/e21050506. URL https://www.mdpi.com/1099-4300/21/5/506.

Joseph T. Lizier. Jidt: An information-theoretic toolkit for studying the dynamics of complex systems. Frontiers in Robotics and AI, 1:11, 2014. ISSN 2296-9144. doi: 10.3389/frobt.2014.00011. URL https://www.frontiersin.org/article/10.3389/frobt.2014.00011.

Michel Loreau and Claire de Mazancourt. Biodiversity and ecosystem stability: a synthesis of underlying mechanisms. Ecology Letters, 16(s1):106–115, 2013. doi: 10.1111/ele.12073. URL https://onlinelibrary.wiley.com/doi/abs/10.1111/ele.12073.

Kohji Mabuchi, Masaki Miya, Yoichiro Azuma, and Mutsumi Nishida. Independent evolution of the specialized pharyngeal jaw apparatus in cichlid and labrid fishes. BMC Evolutionary Biology, 7(1):10, Jan 2007. ISSN 1471-2148. doi: 10.1186/1471-2148-7-10. URL https://doi.org/10.1186/1471-2148-7-10.

Reiji Masuda, Masami Shiba, Yoh Yamashita, Masahiro Ueno, Yoshiaki Kai, Asami Nakanishi, Masaru Torikoshi, and Masaru Tanaka. Fish assemblages associated with three types of artificial reefs: density of assemblages and possible impacts on adjacent fish abundance. Fishery Bulletin, 108(2):162–173, 2010. URL http://aquaticcommons.org/id/eprint/8755.

Alessandro Montalto, Luca Faes, and Daniele Marinazzo. Mute: A matlab toolbox to compare established and novel estimators of the multivariate transfer entropy. PLOS ONE, 9(10):

1–13, 10 2014. doi: 10.1371/journal.pone.0109462. URL https://doi.org/10.1371/journal.pone.0109462.

Camilo Mora, Derek P. Tittensor, Sina Adl, Alastair G. B. Simpson, and Boris Worm. How many species are there on earth and in the ocean? PLOS Biology, 9(8):1–8, 08 2011. doi: 10.1371/journal.pbio.1001127. URL https://doi.org/10.1371/journal.pbio.1001127.

Mark EJ Newman. Power laws, pareto distributions and zipf's law. Contemporary physics, 46(5):323–351, 2005.

Len Nunney. The stability of complex model ecosystems. The American Naturalist, 115 (5):639–649, 1980. URL http://www.jstor.org/stable/2460683. Full publication date: May, 1980.

Vilfredo Pareto. Manual of political economy: a critical and variorum edition. OUP Oxford, 2014.

Stuart L. Pimm. The complexity and stability of ecosystems. Nature, 307(5949):321–326, Jan 1984. ISSN 1476-4687. doi: 10.1038/307321a0. URL https://doi.org/10.1038/307321a0.

Elvira S Poloczanska, Christopher J Brown, William J Sydeman, Wolfgang Kiessling, David S Schoeman, Pippa J Moore, Keith Brander, John F Bruno, Lauren B Buckley, Michael T Burrows, et al. Global imprint of climate change on marine life. Nature Climate Change, 3(10):919–925, 2013.

Hannah Ritchie. Seafood production. Our World in Data, 2019. https://ourworldindata.org/seafood-production.

Thomas Schreiber. Measuring information transfer. Phys. Rev. Lett., 85:461–464, Jul 2000. doi: 10.1103/PhysRevLett.85.461. URL https://link.aps.org/doi/10.1103/PhysRevLett.85.461.

Joseph L. Servadio and Matteo Convertino. Optimal information networks: Application for data-driven integrated health in populations. Science Advances, 4(2), 2018. doi: 10.1126/sciadv.1701088. URL https://advances.sciencemag.org/content/4/2/e1701088.

Lewi Stone. The feasibility and stability of large complex biological networks: a random matrix approach. Scientific Reports, 8(1):8246, 2018. ISSN 2045-2322. doi: 10.1038/s41598-018-26486-2. URL https://doi.org/10.1038/s41598-018-26486-2.

George Sugihara, Robert May, Hao Ye, Chih-hao Hsieh, Ethan Deyle, Michael Fogarty, and Stephan Munch. Detecting causality in complex ecosystems. Science, 338(6106): 496–500, 2012. ISSN 0036-8075. doi: 10.1126/science.1227079. URL https://science.sciencemag.org/content/338/6106/496.

Kentaro S. Suzuki, Keita W. Suzuki, Emi Kumakura, Kana Sato, Yutaro Oe, Tasuku Sato, Hideki Sawada, Reiji Masuda, and Yasuyuki Nogata. Seasonal alternation of the ontogenetic development of the moon jellyfish aurelia coerulea in maizuru bay, japan. PLOS ONE, 14(11):1–22, 11 2019. doi: 10.1371/journal.pone.0225513. URL https://doi.org/10.1371/journal.pone.0225513.

Masayuki Ushio, Chih-hao Hsieh, Reiji Masuda, Ethan R Deyle, Hao Ye, Chun-Wei Chang, George Sugihara, and Michio Kondoh. Fluctuating interaction network and time-varying stability of a natural fish community. Nature, 554:360–363, 2018. doi: 10.1038/nature25504. URL https://doi.org/10.1038/nature25504.

Raul Vicente, Michael Wibral, Michael Lindner, and Gordon Pipa. Transfer entropy—a model-free measure of effective connectivity for the neurosciences. Journal of Computational Neuroscience, 30(1):45–67, Feb 2011. ISSN 1573-6873. doi: 10.1007/s10827-010-0262-3. URL https://doi.org/10.1007/s10827-010-0262-3.

Alejandro F. Villaverde, John Ross, Federico Morn, and Julio R. Banga. Mider: Network inference with mutual information distance and entropy reduction. PLOS ONE, 9(5):1–15, 05 2014. doi: 10.1371/journal.pone.0096732. URL https://doi.org/10.1371/journal.pone.0096732.

Colette C. C. Wabnitz, Vicky W. Y. Lam, Gabriel Reygondeau, Lydia C. L. Teh, Dalal Al-Abdulrazzak, Myriam Khalfallah, Daniel Pauly, Maria L. Deng Palomares, Dirk Zeller, and William W. L. Cheung. Climate change impacts on marine biodiversity, fisheries and society in the arabian gulf. PLOS ONE, 13(5):1–26, 05 2018. doi: 10.1371/journal.pone.0194537. URL https://doi.org/10.1371/journal.pone.0194537.

Peter J Woolf. Chemical Process Dynamics and Controls. openmichigan, 2009.

Can-Zhong Yao and Hong-Yu Li. Effective transfer entropy approach to information flow among epu, investor sentiment and stock market. Frontiers in Physics, 8:206, 2020. ISSN 2296-424X. doi: 10.3389/fphy.2020.00206. URL https://www.frontiersin.org/article/10.3389/fphy.2020.00206.

Figure Captions

Table 1. Indices measuring the relationship between sea temperature and species abundance.

Figure 1. Seasonal fluctuations of sea temperature and α diversity, α diversity over mean temperature. A: The sea surface temperature (red line) and bottom temperature (blue line) over time within the range from June 2002 to April 2014. **B**: Taxonomic α diversity over time. **C**: α diversity over mean temperature (the average of sea surface and bottom temperature). Blue points, light green points, green points, yellow points and red points represent values of α diversity corresponding to different temperature ranges: $\leq$10°C, 10-15°C, 15-20°C, 20-25°C, $\geq$25°C, respectively. Black curve in plot C is a second degree polynomial fitting for α diversity over temperature.

Figure 2. Total species abundance of EP, FS, Native and Invasive groups over time and mean temperature. A: total species abundance of EP (yellow) and FS (blue) groups over time. **B**: total species abundance of Native (yellow) and Invasive (blue) groups over time. **C**: total species abundance of EP (yellow) and FS (blue) groups, abundance of species 1 (green) and 2 (red) over mean temperature on log-log scale. **D**: total species abundance of Native (yellow) and Invasive (blue) groups, abundance of species 1 (green) and 2 (red) over mean temperature on log-log scale.

Figure 3. Exceedance probability distribution, standard deviation vs. mean of species abundance. A: Exceedance probability distribution function (EPDF) are scattered on log-log scale, and fitted by power-law function. $|-\epsilon+1|$ is the exponent of the original power-law function. All exponents for five TR groups are connected by a black dashed line shown in the subplot inside **A**. **B**: standard deviation against mean species abundance is plotted on log-log scale for five TR groups and fitted by power-law function. Here, v is the absolute slope (exponent) of power-law function. All exponents of the scaling law for five TR groups are connected by a black dashed line shown in the subplot inside **B**.

Figure 4. OIF-inferred species interaction networks and matrices. OIF model is used to infer the causal interaction between all pairs of species, yielding interaction (TE) matrices for the whole time series and five TR groups. TE values in interaction matrix are normalized to 1 and drawn in plots A', B', C', D', E' and F'. After removing weak interactions by setting a threshold (0.01) to filter transfer entropy, species interaction networks are reconstructed using *Gephi* and shown in plots A, B, C, D, E and F. The size of node is

proportional to the Shannon Entropy of species, the color of node is proportional to the total outgoing transfer entropy (OTE) of species (the higher the OTE is, the warmer the node's color is.); the width and color of the link between species are proportional to the TE between the pair of species (The higher the TE is, the warmer (wider) the link's color (width) is.).

Figure 5. Exceedance probability distribution function of species interactions after filtering with the threshold 0.01. A, **B**, **C**, **D** and **E**: EPDFs of TE-based interactions between all pairs of species for five TRs: $\leq$10°C, 10-15°C, 15-20°C, 20-25°C, $\geq$25°C. They are shown on log-log scale and fitted by power-law function. In plot **F**, all exponents of the power-law fitting are connected by dashed lines. Scaling exponents for different TR groups are displayed in a coordinate plane where x-coordinates are middle values of temperature ranges (note that 7.5°C and 27.5°C are selected as middle temperature values for the range of temperature lower than 10°C, and higher than 25°C, respectively.), and connected by dashed line from low to high temperature. Note that for the 15-20°C group, EPDF of species interactions presents two regimes that are separately fitted by power-law function. The shape of the connection of exponents therefore presents a bifurcation within the temperature range of 15-20°C.

Figure 6. Distribution of the eigenvalues of TE interaction matrices. Eigenvalues of TE interaction matrices are scattered in a complex plane (five different colors correspond to five TR groups). Dynamical stability of the fish community is computed as the real part of the dominant eigenvalue of TE interaction matrices.

Figure 7. Link salience matrices. Link importance is measured by the algorithm of link salience for all OIF networks corresponding to the whole time series and five TR groups , yielding 15×15 matrices. The values of link salience are normalized to 1, and drawn in plots A, B, C, D, E and F, respectively.

Figure 8. The relationship between the distribution of species abundance and influences. Considering the whole time series of 15 species, ϵ is the slope of the power-law fitting for the EPDF of species abundance (see Fig.S1), TE-base interactions are inferred by OIF model. OTE is interpreted as the total influences of one species on others. Black line is the linear fitting for ϵ vs. OTE of all species.

Species	**TE(T→s_i)**	**TE(s_i→T)**	**MI**	**slope**	**cc**	ρ
Aurelia.sp	0.0233	0.0046	0.3158	0.1369	0.1566	0.0951
Engraulis.japonicus	0.0008	0.0143	0.1323	-0.0820	-0.0656	0.2902
Plotosus.lineatus	0.0292	0.0017	0.1981	0.2771	0.2885	0.3101
Sebastes.inermis	0.0144	0.0313	0.4109	0.0919	0.2783	0.3178
Trachurus.japonicus	0.1712	0.0135	0.6203	0.0658	0.6154	0.6235
Girella.punctata	0.1065	0.0002	0.4721	0.1287	0.4755	0.3847
Pseudolabrus.sieboldi	0.0709	0.0444	0.6913	0.1123	0.7115	0.6902
Halichoeres.poecilopterus	0.0212	0.0073	0.7122	0.0426	0.5055	0.4469
Halichoeres.tenuispinnis	0.0072	0.0063	0.7065	0.0989	0.5011	0.4239
Chaenogobius.gulosus	0.0021	0.0093	0.1274	0.1187	0.1048	0.0634
Pterogobius.zonoleucus	0.0040	0.0011	0.2761	0.1660	0.2584	0.1195
Tridentiger.trigonocephalus	0.0104	0.0244	0.2635	-0.0156	0.1514	0.3158
Siganus.fuscescens	0.0256	0.0101	0.2071	0.2498	0.2433	0.2944
Sphyraena.pinguis	0.0386	0.0049	0.1942	-0.0119	0.2291	0.1992
Rudarius.ercodes	0.0229	0.0153	0.3894	0.0792	0.2369	0.2265

Table 1:

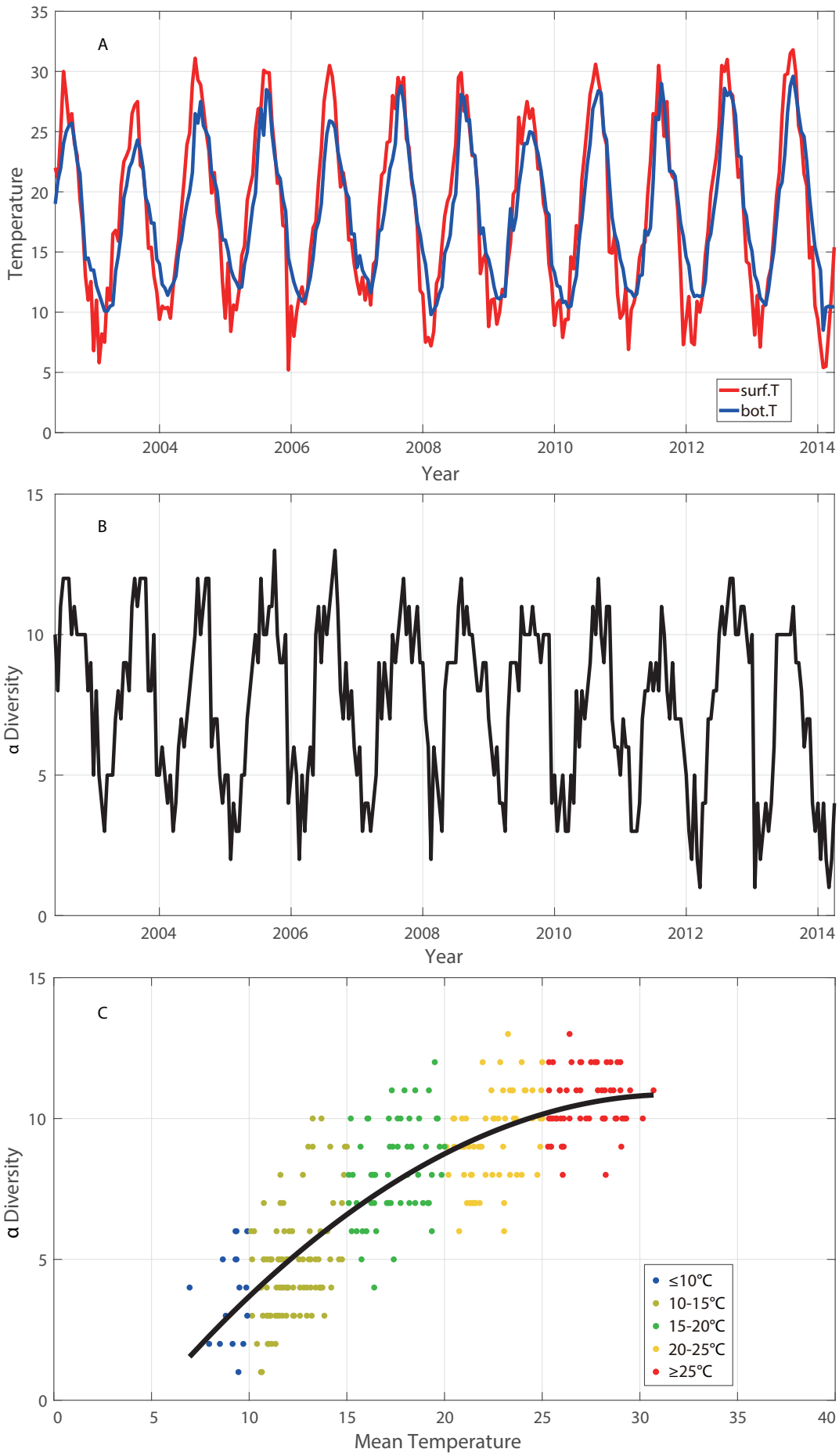
A
Temperature
Year
surf.T
bot.T
B
α Diversity
Year
C
α Diversity
Mean Temperature
≤10°C
10-15°C
15-20°C
20-25°C
≥25°C

Figure 1:

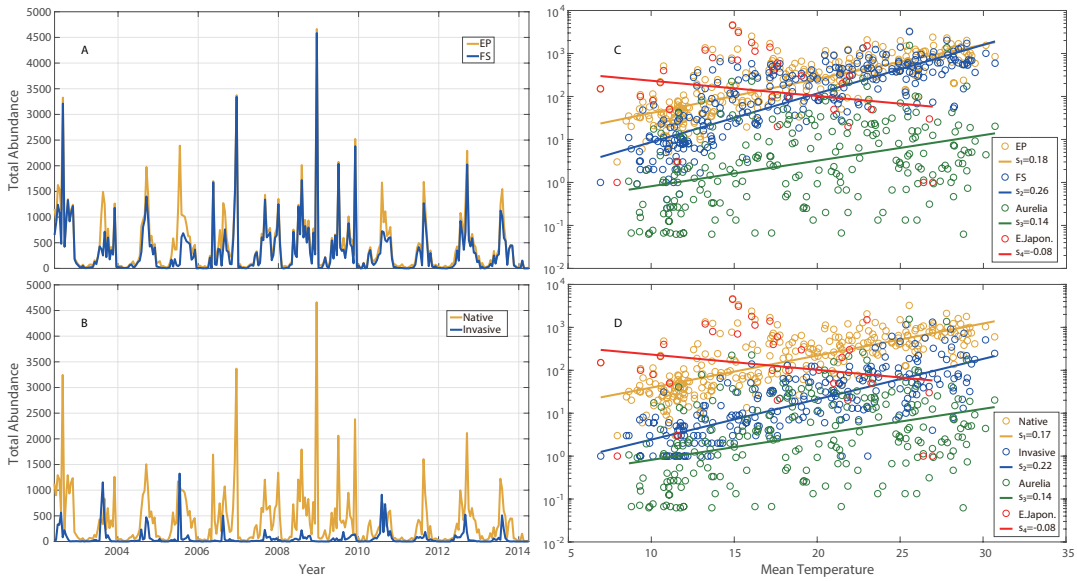
A
EP
FS
Total Abundance
B
Native
Invasive
Total Abundance
Year
C
EP
s1=0.18
FS
s2=0.26
Aurelia
s3=0.14
E.Japon.
s4=-0.08
D
Native
s1=0.17
Invasive
s2=0.22
Aurelia
s3=0.14
E.Japon.
s4=-0.08
Mean Temperature

Figure 2:

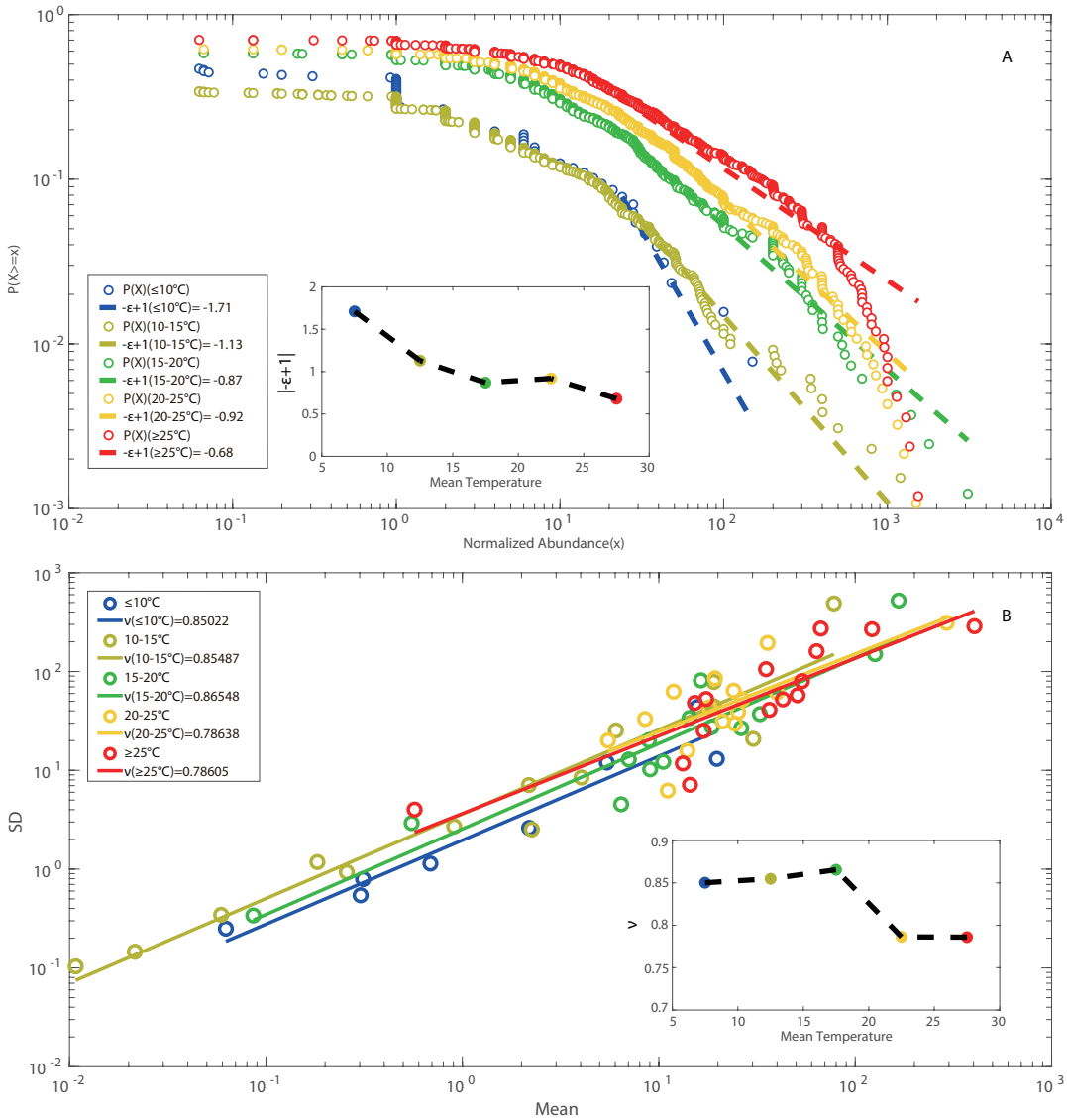
A
P(X>=x)
Normalized Abundance(x)
P(X)(≤10°C)
-ε+1(≤10°C)= -1.71
P(X)(10-15°C)
-ε+1(10-15°C)= -1.13
P(X)(15-20°C)
-ε+1(15-20°C)= -0.87
P(X)(20-25°C)
-ε+1(20-25°C)= -0.92
P(X)(≥25°C)
-ε+1(≥25°C)= -0.68
|-ε+1|
Mean Temperature
B
SD
Mean
≤10°C
v(≤10°C)=0.85022
10-15°C
v(10-15°C)=0.85487
15-20°C
v(15-20°C)=0.86548
20-25°C
v(20-25°C)=0.78638
≥25°C
v(≥25°C)=0.78605
v
Mean Temperature

Figure 3:

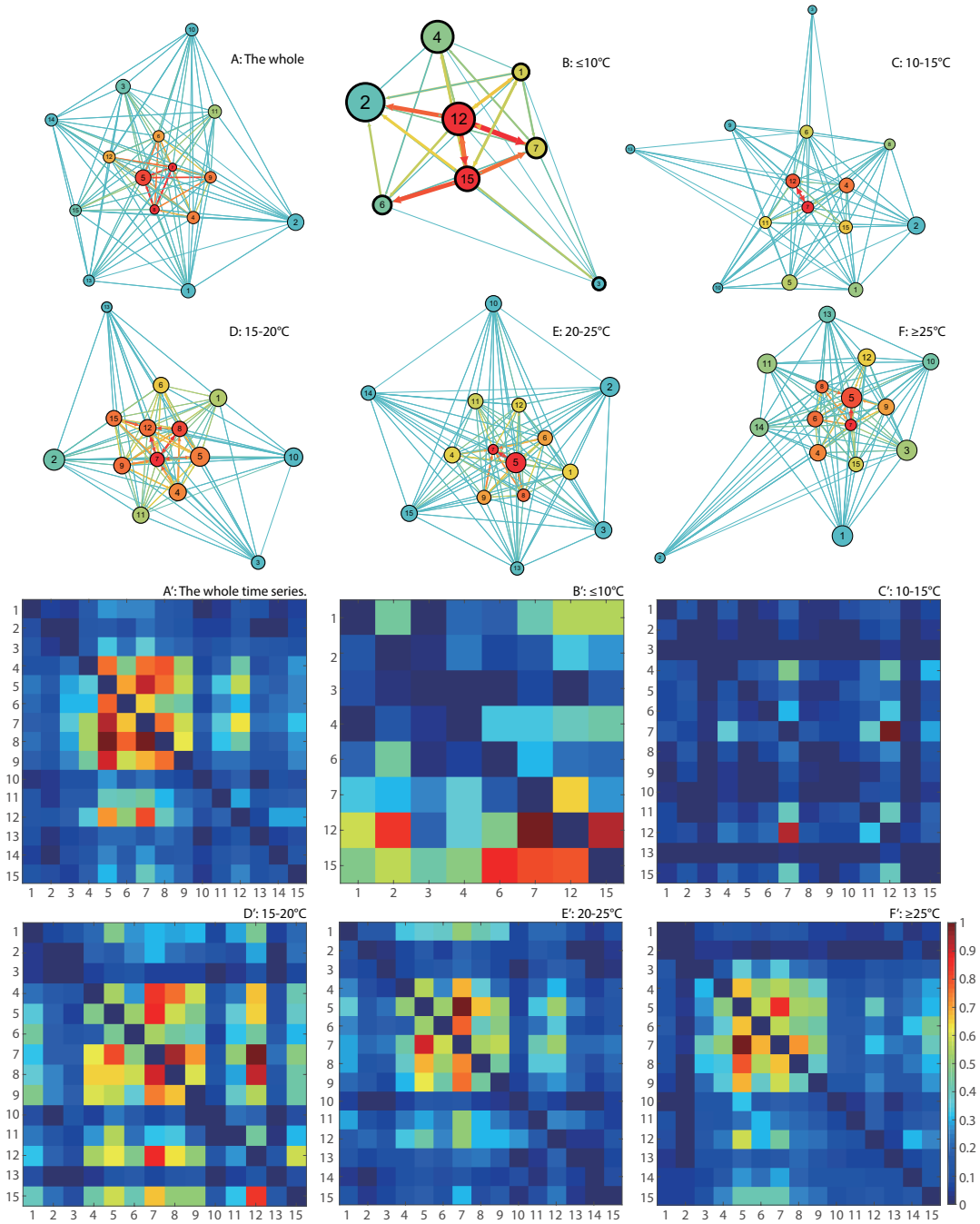
A: The whole
B: ≤10°C
C: 10-15°C
D: 15-20°C
E: 20-25°C
F: ≥25°C
A': The whole time series.
B': ≤10°C
C': 10-15°C
D': 15-20°C
E': 20-25°C
F': ≥25°C

Figure 4:

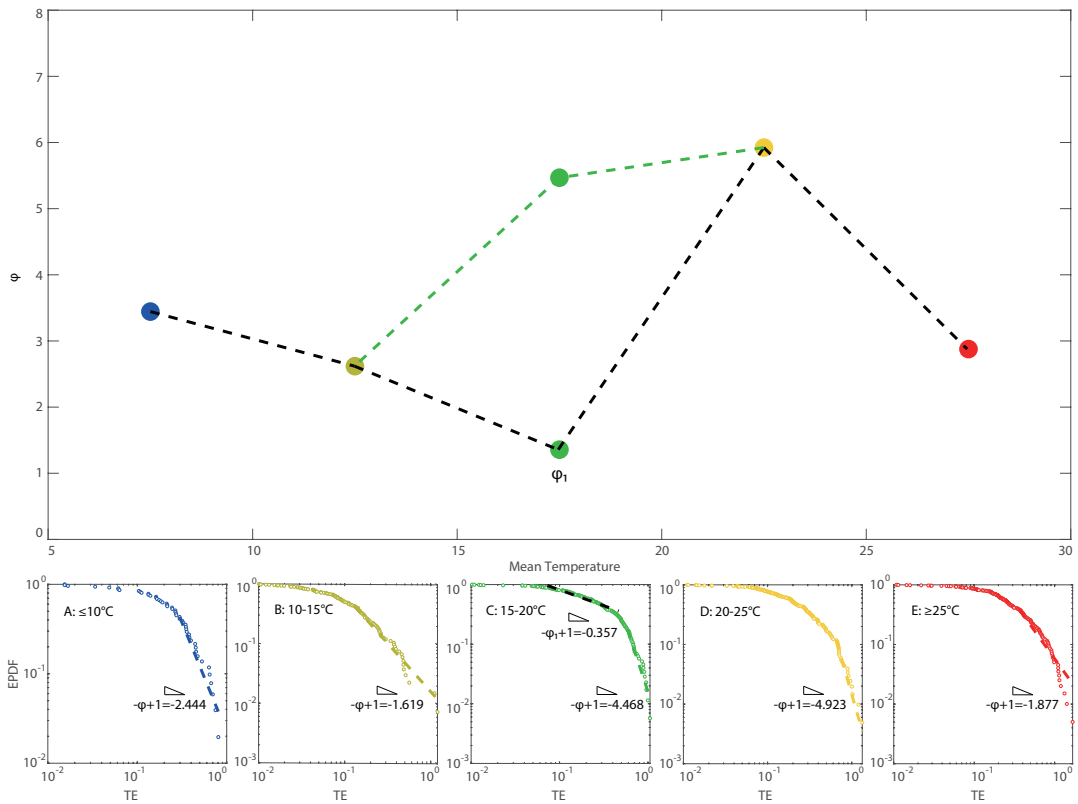
φ
Mean Temperature
φ1
EPDF
TE
A: ≤10°C
-φ+1=-2.444
B: 10-15°C
-φ+1=-1.619
C: 15-20°C
-φ1+1=-0.357
-φ+1=-4.468
D: 20-25°C
-φ+1=-4.923
E: ≥25°C
-φ+1=-1.877

Figure 5:

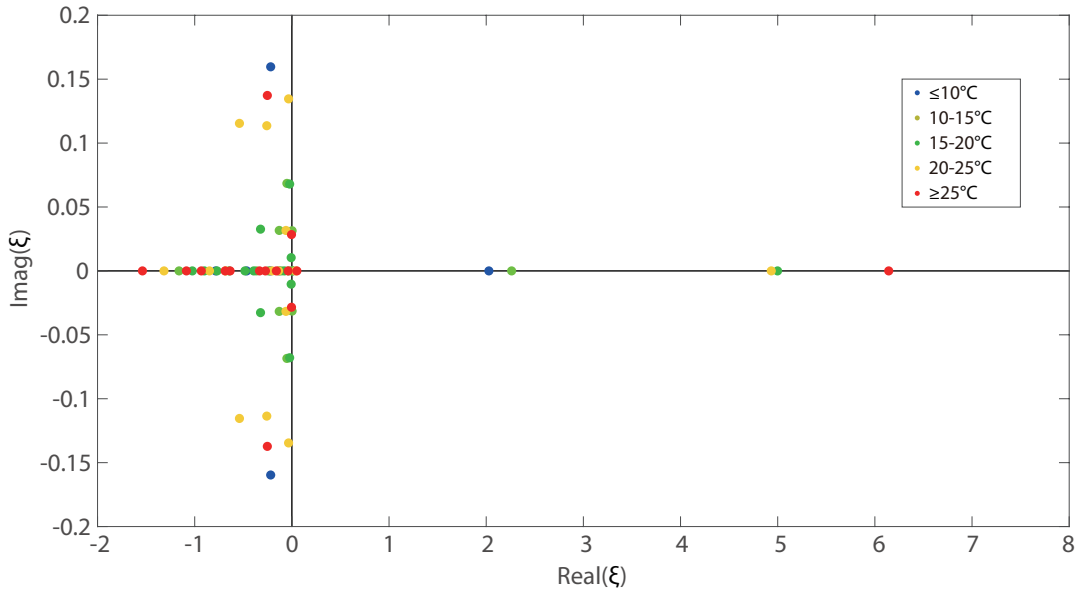
0.2
0.15
0.1
0.05
0
-0.05
-0.1
-0.15
-0.2
Imag(ξ)
-2
-1
0
1
2
3
4
5
6
7
8
Real(ξ)
≤10°C
10-15°C
15-20°C
20-25°C
≥25°C

Figure 6:

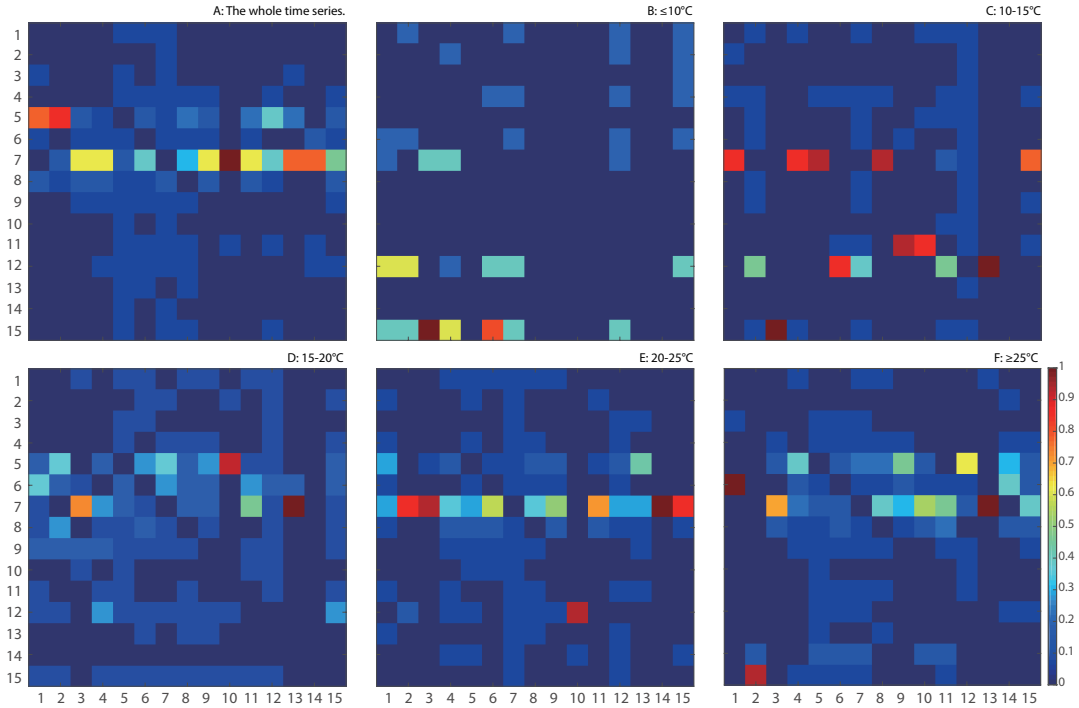
A: The whole time series.
B: ≤10°C
C: 10-15°C
D: 15-20°C
E: 20-25°C
F: ≥25°C
1 2 3 4 5 6 7 8 9 10 11 12 13 14 15
1 0.9 0.8 0.7 0.6 0.5 0.4 0.3 0.2 0.1 0

Figure 7:

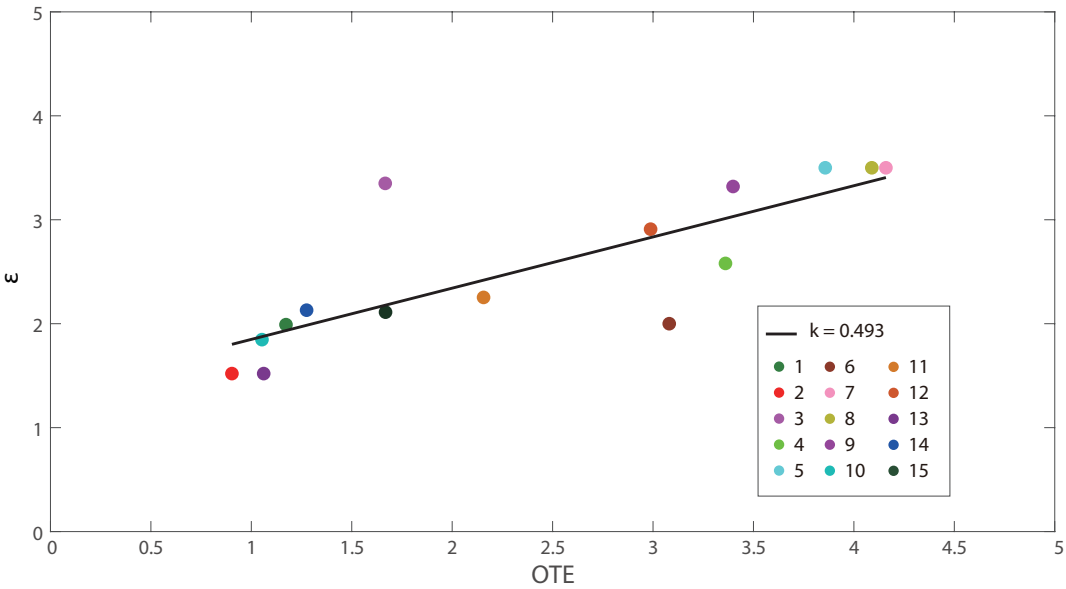
5
4
3
2
1
0
ε
0
0.5
1
1.5
2
2.5
3
3.5
4
4.5
5
OTE
k = 0.493
1
2
3
4
5
6
7
8
9
10
11
12
13
14
15

Figure 8: